

INTRANASAL DEFORMITIES IN DOGS: COMPARATIVE HISTOPATHOLOGY, DIAGNOSTIC  
AND FUNCTIONAL IMAGING

By

Chima Victor Maduka

A THESIS

Submitted to  
Michigan State University  
in partial fulfillment of the requirements  
for the degree of

Comparative Medicine and Integrative Biology—Master of Science

2019

## ABSTRACT

### INTRANASAL DEFORMITIES IN DOGS: COMPARATIVE HISTOPATHOLOGY, DIAGNOSTIC AND FUNCTIONAL IMAGING

By

Chima Victor Maduka

Brachycephalic Airway Syndrome (BAS) is a debilitating condition affecting some of the most populous dogs in the USA. Caused by the developmental foreshortening of the skull, BAS constitutes a major welfare concern as dogs lead an overall poor quality of life. The intranasal component to BAS is poorly understood. It is not clear how intranasal anatomical deformities contribute to the pathophysiology underlying BAS. In this study, we have applied high resolution 3-D imaging (computed tomography) to simulate function (flow pattern) using computational fluid dynamics. Additionally, as part of steps to characterize age-dependent histopathological intranasal changes in brachycephalic dogs, we described the histopathological changes in puppies of French Bulldogs.

This thesis methodically introduces and reviews current literature on BAS while outlining the specific aims, hypotheses and rationale for the study (Chapter 1). Subsequently, the materials and methods used are explained (Chapter 2) and the results are summarized (Chapter 3). The implications of the results, limitations of the study and future directions are discussed (Chapter 4).

Copyright by  
CHIMA VICTOR MADUKA  
2019

To my Mom (Ann Maduka) who gave up her career to nurture my siblings and I, and to my late Dad (Francis Maduka) whose exemplary life keeps me going.

## ACKNOWLEDGEMENTS

I express sincere gratitude to my mentor, Dr. Bryden Stanley. Throughout my Master's program, she patiently taught, supported and encouraged me in a motherly manner. The members of my guidance committee- Dr. André Bénard (Mechanical Engineering), Dr. Nathan Nelson (Radiology), Dr. Stephan Carey (Internal Medicine) and Dr. Jack Harkema (Pathology) provided me with multidisciplinary and invaluable insight. Other significant contributors and collaborators include Dr. Christopher Contag, Dr. Kurt Williams, Dr. Dalen Agnew, Ashleigh Tindle, Volkan Yildirim, Drs. Claire and Kurt Hankenson, Ryan Lewandowski, Dr. Sina Mamouri and the MSU Histopathology, to whom I owe many thanks. I would like to express deepest gratitude to Dr. Vilma Yuzbasiyan-Gurkan. As both Director of the Comparative Medicine and Integrative Biology (CMIB) graduate program and Associate Dean for Research and Graduate Studies, her motherly support was second to none. The Graduate Program Coordinator, Dimity Palazzola, has always been incredibly supportive and happy to help with any challenge I encountered.

The Mastercard Foundation provided the full scholarship that covered all my fees and expenses. Financial support for my research came from Michigan State University (MSU) College of Veterinary Medicine (CVM) and Dehn Endowed Funds, for which I am grateful.

My mum, niece (Mmachi) and siblings (Eucharika, Franklyn, Kambili, Obinna) are the celebrities in my life. Alongside their families, Dr. Chuks Onah, Rev. Fr. Sunday Ikpe and Prof. Ikechukwu Igbokwe, have made numerous sacrifices toward my success story. To all my friends who've stood by me, I say thank you. Lastly but most importantly, my heartfelt praise goes to God Almighty, in whom I live and move and have my being.

## TABLE OF CONTENT

<b>LIST OF TABLES</b>	viii
<b>LIST OF FIGURES</b>	ix
<b>CHAPTER 1: Introduction and Literature Review</b>	1
INTRODUCTION	2
DEVELOPMENTAL ANATOMY OF THE CANINE SKULL	3
PATHOPHYSIOLOGY OF BRACHYCEPHALIC AIRWAY SYNDROME (BAS)	5
CONDITIONS AND CLINICAL SIGNS ASSOCIATED WITH BRACHYCEPHALIC AIRWAY SYNDROME	6
DIAGNOSTIC IMAGING OF THE UPPER AIRWAY OF DOGS	7
TREATMENT AND PROGNOSIS OF BRACHYCEPHALIC AIRWAY SYNDROME (BAS)	8
THE ANATOMY OF THE NASAL CAVITY	9
MODELING OF THE UPPER AIRWAYS	10
FUNCTIONAL IMAGING OF THE UPPER AIRWAYS	11
INTRANASAL HISTOLOGY	13
OVERALL GOAL	14
HYPOTHESES	15
SPECIFIC AIMS	15
<b>CHAPTER 2: Materials and Methods</b>	18
STUDY 1	19
Patient Selection	19
CT Examination and Nasal Measurements	19
Statistical Analysis	22
STUDY 2	23
Animals	23
Histopathology	23
Nasal morphometry	24
Statistical analysis	24
STUDY 3	25
Functional Imaging (Computational Fluid Dynamics simulation)	25
Statistical analysis	26
<b>CHAPTER 3: Results</b>	27
STUDY 1	28
STUDY 2	32
STUDY 3	32
<b>APPENDIX</b>	33
<b>CHAPTER 4: Discussion and Conclusion</b>	47
STUDY 1	48

STUDY 2	51
STUDY 3	54
LIMITATIONS AND FUTURE PERSPECTIVE	56
CONCLUSION	57
<b>APPENDIX</b>	59
<b>REFERENCES</b>	70

## LIST OF TABLES

<b>TABLE 4.1:</b> Characteristics of dogs enrolled in the study.	34
<b>TABLE 4.2:</b> Comparison of the nasal cavity of mesaticephalic and brachycephalic of dogs.	35
<b>TABLE 4.3:</b> Comparison of nasal cavity statistic in mesaticephalic and brachycephalic dogs after normalizing to skull length-width (LW) index and body weight (BW).	36
<b>TABLE 4.4:</b> Variation of the nasal cavity among enrolled brachycephalic breeds.	37
<b>TABLE 4.5:</b> Comparison of nasal cavity statistic among enrolled brachycephalic breeds after controlling for skull length-width (LW) index and body weight (BW).	38
<b>TABLE 4.6:</b> Effect the presence of septal deviation and aberrant turbinate have on the nasal cavity.	39
<b>TABLE 4.7:</b> Effect the presence of septal deviation and aberrant turbinate have on the nasal cavity after controlling for skull length-width (LW) index and body weight (BW).	40
<b>TABLE 4.8:</b> Distribution of the types of epithelium in the nasal cavity of puppies by histomorphometry.	41
<b>TABLE 4.9:</b> Comparison between wall shear stress, airway resistance and pressure drop in the nasal cavities of brachycephalic and mesaticephalic dogs.	42

## LIST OF FIGURES

<b>FIGURE 1a:</b> Relationship between body weight and measurements in the nasal cavity of mesaticephalic dogs.	43
<b>FIGURE 1b:</b> Relationship between body weight and measurements in the nasal cavity of brachycephalic dogs.	44
<b>FIGURE 1c:</b> Relationship between age and measurements in the nasal cavity of mesaticephalic dogs.	45
<b>FIGURE 1d:</b> Relationship between length-width index and measurements in the nasal cavity of mesaticephalic dogs.	46
<b>FIGURE 2:</b> Anatomical landmarks for preoperative assessment of CT images of the nasal cavity.	60
<b>FIGURE 3:</b> The major histopathological characteristics of sections (T1-T8) of the nasal cavity in different dog breeds.	63
<b>FIGURE 4:</b> Flow pattern showing velocity gradients in a mesaticephalic dog (a), French bulldog (b), English bulldog (c) and Pug (d). As velocity increases pressure decreases (Bernoulli equation).	67
<b>FIGURE 5:</b> Smooth 3-D image showing the inlet (a) and outlet (b) formed by the nares and nasopharyngeal meatus, respectively, in a mesaticephalic dog; inlet and outlet of a brachycephalic dog are shown in (c) and (d), respectively.	68
<b>FIGURE 6:</b> Histopathological sections (T1-T8) from the incisive papilla to the soft palate at the level of the nasopharyngeal meatus.	69

## **CHAPTER 1: Introduction and Literature Review**

## **INTRODUCTION**

Skull shapes are described as being brachycephalic (short, wide-headed), mesaticephalic (medium proportions) or dolichocephalic (long, narrow-headed)<sup>1</sup>. Long-term breeding for brachycephaly has resulted in dogs and cats having shortened muzzle and wide orbits that markedly differ from their mesaticephalic and dolichocephalic counterparts. Brachycephalic dogs have craniofacial index of less than 0.23 and a skull length-width (LW) index of less than 1.44.<sup>1,2</sup> Brachycephalic breeds possess a plethora of unique anatomical disorders, which may occur in combination or separately, and which can cause varying degrees of air turbulence and airway obstruction.<sup>3,4</sup> These primary anomalies include stenotic nares with large and less mobile cartilaginous nasal wings; elongated and thickened soft palate; excessive nasal conchae with rostral and caudal aberrant turbinates; nasal septal deviation; tracheal hypoplasia and thickened mucosa at the level of the soft palate.<sup>4-7</sup> The turbulent airflow and partial obstruction from these primary anatomical abnormalities frequently cause secondary changes which further exacerbate the airway obstruction including pharyngeal edema; edematous nasal conchae; laryngeal mucosal edema, edematous and everted laryngeal ventricles, laryngeal collapse (of cuneiform and corniculate processes of the arytenoid) and less commonly tracheal and bronchial collapse.<sup>4,6,8-21</sup> The resulting airway obstruction characterizes the debilitating and progressive course of brachycephalic airway syndrome (BAS). Brachycephalics have also been noted to have a higher incidence of hypertrophic and inflamed tonsils, often noted to be outside of the tonsillar crypt.

BAS constitutes a significant welfare issue because ownership of brachycephalics is increasing and public education on the impact of BAS on their pet's quality of life is limited.<sup>22</sup>

Affected dogs are distributed worldwide. In the USA, English and French bulldogs are now (2018) the 4th and 5th most populous dogs.<sup>23</sup> Brachycephalic dog breeds most affected by BAS include the English and French bulldog, pug, pekingese, shih tzu, Boston terrier, Cavalier King Charles spaniel, boxers, Dogue de Bordeaux, Miniature Bull Terriers, Staffordshire Bull Terriers and bullmastiffs.<sup>4,9,12,15,17,22,24-27</sup> BAS is most prevalent among pugs, English and French Bulldogs.<sup>9,12,15,25-27</sup> Some breeds such as Norwich terrier, golden retriever, spaniel and dachshund present with upper respiratory disorders similar to BAS, but these remain to be definitively characterized.<sup>3,25,28,29</sup>

## **DEVELOPMENTAL ANATOMY OF THE CANINE SKULL**

The embryology of the dog skull has been described<sup>1</sup>. The roof of the skull (calvaria) is formed by membranous ossification of the paired frontal and parietal bones and a single, more superficial interparietal bone from the fetal desmocranium, dorsal to the brain. Alongside the olfactory, optic and otic sensory capsules, the base of the skull (basicranium) composed of the basioccipital, basisphenoid, presphenoid and ethmoid bones (and conchae) form from the chondrocranium. This chondrocranium arises from the parachordal and trabecular cartilages which, together with the branchial cartilage, originate from the neural crest ectoderm.<sup>1,6</sup> Deficiency and early ankylosis of cartilaginous matrix that ossifies to form the base of the skull underlies the shortened basicranial axis inherent in brachycephalic dogs.<sup>1,3</sup> Definitive bone formation occurs by membranous or endochondral ossification or both. In addition, although bones formed from either process are structurally similar, membranous ossification precedes endochondral ossification. Consequently, the dentary of the mandibles, nasal, frontal, parietal, zygomatic, maxilla, palatine and other membranous-

formed bones ossify earlier than cartilages of the jaws, hyoid apparatus, ear ossicles and other cartilaginous-derived bones. The basisphenoid and presphenoid bones laterally fuse with the alisphenoid and orbitosphenoid bones to form the basisphenoid with temporal wings and presphenoid with orbital wings, respectively, that comprise the sphenoidal complex. The sella turcica which encloses the pituitary gland is formed by the basisphenoid and clinoid process, whereas, below the cribriform plate, the lateral ethmoids combine to form the sphenethmoids and the mesethmoid gives rise to a median perpendicular plate. The intersphenoidal synchondrosis is the joint formed by presphenoid and basisphenoid, whereas, the spheno-occipital synchondrosis is the joint between the basisphenoid and basioccipital.

Premature union of either the intersphenoidal or spheno-occipital synchondrosis restricts lengthening along the skull along the basicranial axis. This is prevalent among brachycephalic breeds and manifests as disproportionate upper and lower jaws, creating a relative mandibular prognathism and maxillary brachygnathism. In addition, because endochondral ossification precedes membranous ossification, nasal conchae extend into the nasopharyngeal meatus because of the restricted space in the already formed nasal capsule.<sup>6,9</sup> In some cases, aberrant post-natal growth of the medial nasal turbinates does occur as rostral aberrant turbinates (RAT) when they project into the alar region<sup>6</sup>. The aberrant growth of the medial and ventral nasal turbinates through the chonane into the nasopharygeal meatus has been designated caudal aberrant turbinates (CAT)<sup>6,12-14</sup> and are more commonly associated with brachycephalic than mesaticephalic dogs.<sup>30</sup> The presence of nasal septal deviations in both mesaticephalic and brachycephalic dogs have been documented but their effect on airway obstruction is uncertain.<sup>12,30</sup> However, using

computed tomography and computational fluid dynamics in humans, association has been established between septal deviation and airway resistance.<sup>13,31,32</sup> The sequence of development of the skull is from the bones of the face and calvaria to the bones of the basicranium, sensory capsules and hyoid apparatus. In the supraorbital, pterygoid and temporal bones, membranous and endochondral ossification concurrently occur. Sphenoidal ossification progresses from the temporal wings to the body of sphenoid, preoptic root of orbital wings, metoptic root and body of presphenoid.

### **PATHOPHYSIOLOGY OF BRACHYCEPHALIC AIRWAY SYNDROME (BAS)**

The foreshortening of the brachycephalic skull is not accompanied by commensurate reduction in the size of the soft-tissues therein, leading to altered nasopharyngeal anatomy.<sup>9,33</sup> Whereas in mesaticephalic dogs, passive exhalation of air normally results in slightly negative pleural pressure, in brachycephalic breeds, exhalation is an active process involving accessory muscles of respiration and resulting in steep changes in pleural pressure.<sup>34,35</sup>

In mesaticephalics, the nose, larynx and lower airways contribute 76.5 %, 4.55% and 18.95% of total airway resistance, respectively.<sup>36</sup> Primary abnormalities of BAS including stenotic nares, macroglossia, elongated and thickened soft palate, nasal septal deviation, rostral and caudal aberrant turbinates and hypoplasia of the trachea and bronchi, lead to marked non-linearity in the airway passages, elevated luminal resistance and greater respiratory effort.<sup>3,16,36</sup> Greater inspiratory effort involves generating significant negative pressure that can compress the collapsible airway lumen and cause eversion of structures due to marked pressure gradients across the luminal walls (transmural pressure).<sup>4,9,10,34</sup>

This process results in the secondary anatomical disorders including mucosal edema across the airway passages, tonsillar and laryngeal saccule eversion, collapse of the larynx, trachea and bronchi. Combining their non-linear effects, primary and secondary abnormalities increase obstruction, turbulence and velocity of air within the respiratory tract, thereby, decreasing airway pressure in accordance with Bernoulli's principle that defines an inverse relationship between pressure and velocity. Further negative pressure necessitates greater respiratory effort and collapse of airway structures. Like a positive feedback mechanism, this cycle progresses leading to hypercapnia. Thus, early identification and surgical intervention is important to improve quality of life and prevent life-threatening obstruction.<sup>10,17,37</sup>

In addition, the upper airway is enriched with neurons that innervate muscles and maintain muscle tone.<sup>38</sup> Therefore, conditions that affect the electromyogram (EMG) of pharyngeal dilator muscles, including tensor palatini, levator palatini, and genioglossus, will affect airway patency and resistance.<sup>39-41</sup> In humans, upstream nasal resistance within the nasal airway, obesity, gender, surface adhesive forces, tracheal tug, hormonal status, neck and jaw posture and age have been implicated as factors affecting upper airway resistance.<sup>38</sup>

## **CONDITIONS AND CLINICAL SIGNS ASSOCIATED WITH BRACHYCEPHALIC AIRWAY SYNDROME**

Hiatal hernia, lung lobe torsion and a complex of gastroesophageal and duodenal disorders such as retching, vomiting and regurgitation have been reported in brachycephalic dogs and cats.<sup>3,9,24,27,34,42</sup> Recent epidemiological studies have shown that brachycephalic airway syndrome (BAS) is associated with higher prevalence of middle ear lesions, hypomagnesemia, vertebral malformations, bowed limbs, cleft lip, cleft palate and ocular

disorders.<sup>43-49</sup> In addition, the burden of brachycephaly includes sleep disorders, asphyxiation, decrease in left ventricular systolic performance, severe exercise intolerance, marked sensitivity to heat stress and prolonged recovery time after physical exercise, impairing the overall quality of life.<sup>8,16,50,51</sup> Other signs of BAS are snoring, inspiratory dyspnea, gagging, increased respiratory effort, stridor, hyperthermia, cyanosis, tachypnea, stertor, abducted forelimbs, syncope and death in more severe cases.<sup>4,8,9,15,16,22,34,51,52</sup>

### **DIAGNOSTIC IMAGING OF THE UPPER AIRWAY OF DOGS**

Clinically, diagnosis of brachycephalic airway syndrome (BAS) can be made by signalment, history of exercise intolerance, sleep apnea, gastroesophageal disorders during respiratory distress, snoring and other signs of BAS, physical and clinical examinations that connote airway obstruction and imaging.<sup>9,51</sup> Many imaging modalities can be used in various combinations to investigate airways obstruction in brachycephalic airway syndrome (BAS). Radiography, fluoroscopy, endoscopy, computed tomography and magnetic resonance imaging, have been used by various studies to determine cephalometric indices and evaluate dimensions of upper or lower airway abnormalities of brachycephalic dogs and cats.<sup>6,12,18,26,53-58</sup> Radiography reveals heart and lung involvement while computed tomography provides for detailed assessment of the nostrils, vestibule, nasal cavity, and nasopharynx and oropharynx for preoperative planning and endoscopy of the upper airways.<sup>9,12-14</sup> In contrast to lateral radiography and cephalometry, high resolution computed tomography and magnetic resonance imaging allow evaluation in transverse, dorsal and sagittal planes.<sup>59</sup> Moreover, computed tomography and magnetic resonance

imaging provide data that may be used for dynamic (functional) simulation of the upper airways.

### **TREATMENT AND PROGNOSIS OF BRACHYCEPHALIC AIRWAY SYNDROME (BAS)**

The goal of medical or surgical intervention in brachycephalic patients is relief of upper airway obstruction after patient stabilization.<sup>9</sup> Surgical treatment options include amputation of the ala nasi, various aplasty techniques (wedge and punch resections), alapexy and vestibuloplasty to improve airflow through the stenotic nares; removal of malformed parts of the ventral and medial nasal conchae to relieve intranasal obstruction; staphylectomy and a folded flap palatoplasty for the soft palate, laryngeal sacculotomy to resect everted ventricles, partial arytenoidectomy, tonsillectomy and permanent tracheostomy.<sup>9,12-14,17,60</sup> Although there are instances where long-term recurrence of clinical signs have been reported, dogs suffering from brachycephalic syndrome benefit from surgery, with reduced mortality rates.<sup>4,10,27</sup> Prognostic factors include the degree of primary and secondary abnormal anatomy, age of the animal to prevent development of secondary signs, body condition and employed surgical technique.<sup>16,17,61</sup>

## **THE ANATOMY OF THE NASAL CAVITY**

The wings of the nares are supported by the paired dorsolateral cartilages, whereas, the floor and lateral wall of the nasal vestibule are shaped by the ventrolateral and septal nasal cartilages.<sup>62</sup> The dorsolateral nasal cartilage articulates with the nasal bone by dorsolateral nasal ligament. The lateral nasal ligaments provide support laterally and the accessory nasal cartilages provides additional support to the ventral aspect of the nose.<sup>62</sup> The nasal cavity extends from the external nares to the choanae, longitudinally divided by the nasal septum. Rostrally, the nasal septum is cartilaginous but caudally it becomes bony and extends to articulate with the cribriform plate to form the crista galli.<sup>1,62,63</sup> The cribriform plate demarcates the nasal cavity from the cranial cavity.<sup>1</sup> The division of the nasal cavity is normally symmetrical and each cavity is rostrally and caudally occupied by the ventral nasal conchae and ethmoturbinates, respectively.<sup>1,64</sup> The conchae are denser rostrally and interspersed with more air spaces caudally.<sup>64</sup> The tortuous conchae in the nasal cavity may make contact as intraconchal, interconchal and septoconchal mucosal contact points, which have narrow air passages.<sup>33,65,66</sup> They are more prevalent in brachycephalic dogs than mesaticephalic dogs.<sup>30</sup>

The ethmoid bone consists of the cribriform plate which serves to attach the ethmoturbinates, a median perpendicular plate and two ethmoidal labyrinth.<sup>1</sup> The bony nasal septum is formed by the median perpendicular plate that fuses with the vomer ventrally and septal processes of the frontal and nasal bones dorsally. The dorsal nasal meatus is above the dorsal nasal conchae, whereas, the ventral nasal meatus is below the ventral nasal conchae. However, the middle nasal meatus is the cleft between the dorsal and larger ventral nasal conchae.<sup>1</sup> The ventral nasal concha terminates rostrally as the alar fold

and the common nasal meatus is the air passage on either side of the nasal septum. The air passage from the caudal end of each side of the nasal cavity to the pharynx constitutes the nasopharyngeal meatus; and the rostral portion of nasopharyngeal meatus is termed the choanae (internal nares).<sup>62,63</sup>

The ethmoturbinates, which attach caudally to the cribriform plate and ventrally to the basal laminae, are bony scrolls divided into four long ventral endoturbinates and six smaller dorsal ectoturbinates.<sup>1</sup> The first endoturbinate is the longest and arises from the dorsal aspect of the cribriform plate and the medial part of the roof plate. The first endoturbinate rostrally attaches to the medial aspect of the nasal bone as the dorsal nasal conchae.<sup>1</sup> In the caudal and ventral nasal cavity, the ethmoidal conchae are outgrowths from the ethmoid bone which extend into the frontal sinus. Together, the maxillary recess, sphenoidal sinus and the frontal sinus comprise the paranasal sinuses.<sup>62</sup> In brachycephalic breeds, the nasal bone is particularly short and grooved on the ventral aspect of its rostral half, forming the dorsal nasal meatus.<sup>1</sup>

## **MODELING OF THE UPPER AIRWAYS**

The lack of objective measures of BAS surgical efficacy has been reported.<sup>18</sup> Studies have relied on subjective assessments by assigning clinical scores.<sup>67</sup> Therefore, physical and mathematical models have emerged to study pressure-flow relationships and resistance of the upper airways in dogs.

The normal upper airway of dogs is collapsible and dynamic, similar to the human upper airways due to intraluminal and extraluminal pressure changes.<sup>38</sup> Rhinomanometric studies measuring solely nasal airflow resistance (excluding the influence of nares and vestibulum)

confirmed that intranasal resistance is significantly higher in brachycephalic dogs compared with normal dogs.<sup>68</sup> Barometric whole body plethysmography using a pneumotachograph and oesophageal balloon technique has been used to evaluate upper airway obstruction in dogs.<sup>37,61,68-70</sup> In human studies of airway obstruction and surgical efficacy, acoustic rhinometry, nasal spirometry, rhinostereometry, Starling resistor model and rhinomanometry which measure pressure-flow relationship.<sup>38,71,72</sup> Recently, more objective methods of appraising airflow resistance by functional imaging (computational fluid dynamics) simulations of the upper airway have been used.

### **FUNCTIONAL IMAGING OF THE UPPER AIRWAYS**

The upper airway physiology of canine models has been studied using computational fluid dynamics (CFD), mostly after a high resolution magnetic resonance imaging (MRI) scan, to simulate odorant and sniffing mechanisms.<sup>58,73-75</sup> In the horse cadaver, computational fluid dynamics has been used after computed tomography (CT) to simulate the in vivo geometry of the upper airway.<sup>76</sup> A recent study by Hostnik et al<sup>18</sup> evaluated nasal resistance in the upper airway of English Bulldogs. No studies have compared nasal resistance in brachycephalic and mesaticephalic dogs using CFD.

In obstructive sleep apnea syndrome (OSAS), the use of computed tomography and computational fluid dynamics have been validated as diagnostic tools to investigate upper airway obstruction.<sup>59,77-87</sup> For extraction of visual data and CFD simulations of the upper airway, conversion of acquired three-dimensional (3-D) CT images to computer aided design (CAD) models using commercial software programs, such as MIMICS, is required.<sup>59</sup> Segmentation of digital imaging and communications in medicine (DICOM) images involves

selective partitioning of a digital image to delineate areas of interest. Image segmentation is based on Hounsfield units (HU) assigned to each pixel (or voxel) on DICOM images, such that pixels with the same range of Hounsfield units look alike but differ from pixels of different Hounsfield units.<sup>77</sup> The Hounsfield unit is a measure of the radiodensity of tissues, ranging from -1024 to 3071.<sup>81</sup> Assigning threshold levels to extract areas of an image, such as -1024 to -450 HU (or -226 HU) delineates the boundary of air for the upper airways<sup>18,77,80</sup> giving rise to 3-D CAD models. For high contrast segmentation of the airway using volume rendering, inversion of 3D-rendered image is used, such that negative values change to positive values and vice versa.<sup>83,87</sup> Models that are based on cubic pixels (voxels) may exhibit staircasing effect necessitating an appropriate smoothing algorithm with volume compensation that will not lose patient-specific features.<sup>77,87</sup> Afterwards, anatomic geometry or parameters, including volume, length, cross-sectional area (volume/ length) and minimal cross-sectional area at different levels of the patient's upper airway can be deduced. Thereafter, the 3-D CAD model is divided into discrete tetrahedral cells to construct numerical (computational) mesh (domain, grids or cells), typically consisting of 500,000 to 1,600,000 computational grids<sup>59,77,81,82</sup> using MIMICS or CFD pre-processing commercial software, such as ICEM-CFD. Since a greater number of grids leads to a more accurate description of flow behavior, selective numerical increment of grids in regions of interest for higher resolution is common.<sup>59,86</sup>

The 3-D computational mesh is imported into the CFD commercial software, such as FLUENT, usually in stereolithographic or matrix laboratory file formats.<sup>18,80,83,87</sup> Several airway flow-governing, discretized equations (models) can be solved by FLUENT such as the steady Reynolds Averaged Navier-Stokes (RANS), Continuity, elliptic staggered, unsteady

Large Eddy Simulations (LES), Spalart-Allmaras model, k- $\epsilon$  and k- $\omega$  Shear Stress Transport (SST) turbulence equations.<sup>18,77,80-84,87</sup> Because dependent variables exceed the governing equations, it is common to use the equations of state to match dependent variables with governing equations.<sup>86</sup> However, certain boundary conditions must be fixed after defining the inlet and outlet, depending on the direction of air flow during inspiration or expiration, and may be sourced from literature. Boundary assumptions include pressure inlet (for the nostril, ambient atmospheric pressure (1 atm or 0 atm has been used<sup>18,70,81,82,86</sup>), velocity inlet, pressure outlet (pneumotach measurements at the caudal end of the nasal passages, for nasal studies, have been used), no-slip wall condition, laminar or turbulent flow, volume of air at peak inspiration and expiration, homogenous air density and Newtonian viscosity and incompressible air condition (fixed inlet velocity = fixed inlet flow mass rate) which can be verified by low (<0.3) Mach number.<sup>77-84,86-88</sup> Simulations are repeated until convergence of the mass flow rate (residuals < 0.2%) is achieved.<sup>77,83,87</sup> From the outcome of the CFD analysis, the following parameters for different regions of the upper airway can be obtained: Pressure drop (change or difference,  $\Delta P$ ), mass flow rate (m), resistance ( $\Delta P/m$ ), intraluminal pressure at the smallest cross-sectional area, wall shear stress, density, energy and temperature.

## **INTRANASAL HISTOLOGY**

Due to advances in 3-D imaging, including CT and MRI, there are indications that both congenital and acquired intranasal abnormalities may have critical roles in the pathophysiology of brachycephalic airway syndrome (BAS)<sup>58</sup> Some of these anatomical abnormalities include aberrant nasal turbinates, increased mucosal contact points,

submucosal edema and the presence of abnormal amounts of mucus.<sup>6,14,65</sup> The histology of the soft-palate is well characterized.<sup>7,89</sup> The nasal mucosa of mesaticephalic breeds has been described using histochemistry and scanning electron microscopy.<sup>90,91</sup> However, to date, there are no histological studies on age-dependent intranasal pathologic changes in brachycephalic dogs compared to mesaticephalic breeds. Describing the intranasal histopathologic features that characterize brachycephaly relative to mesaticephalic dogs, and subsequently elucidating altered mechanisms associated with BAS will reveal new ways to manage the condition. Additionally, understanding the age-dependent pathologic developmental changes in the nasal cavity of brachycephalic dogs, may provide insight to similar investigations regarding the intranasal contribution to obstructive sleep apnea syndrome in humans.

## **OVERALL GOAL**

The overall goals of this study were to:

- Better correlate intranasal abnormalities of structure with function in BAS patients and validate CT as a potentially useful screening test in these patients (Study 1)
- Map the intranasal epithelium in mesaticephalic and brachycephalic dog breeds, and document age- and breed- dependent changes with maturation (Study 2)
- Optimize computational fluid dynamics to describe the flow pattern in BAS patients, relative to mesaticephalic dogs, and identify identifying surgical targets within the nasal cavity by correlating intranasal abnormalities with airway resistance (Study 3)

Our **long-term goal** is to improve pre-operative assessment of brachycephalic dogs that suffer from BAS, to guide the surgeon's decision regarding the best treatment option for BAS patients on a case-by-case basis.

## **HYPOTHESES**

We hypothesized that:

- The volume of tissue within the part of the nasal cavity involved with respiration (and dynamic air flow) will be higher in brachycephalic than mesaticephalic dogs (Study 1)
- There will be significant histopathological changes in both cell type and distribution, of the intranasal epithelium of different breed types (brachycephalic, mesasticephalic, Norwich terriers) (Study 2)
- Computational fluid dynamics can be optimized to determine areas of extreme pressure and velocity changes in the nasal cavity of BAS patients and evaluate nasal airway resistance in dogs; and the intranasal resistance, shear stress and pressure drop in brachycephalic dogs will be higher when compared with mesaticephalic dogs (Study 3)

## **SPECIFIC AIMS**

A. Study 1 on CT images of the nasal cavity aimed to:

- Measure the relative contribution of the frontal sinus, maxillary recess and functional respiratory air volumes to total air in mesaticephalic and brachycephalic dogs

- Measure the relative contributions of air and tissue to the compartment of the nasal cavity involved with respiration (dynamic air flow) in mesaticephalic and brachycephalic dogs
- Measure volume to cross-sectional area at specific anatomical levels to relate intranasal abnormal structure to dysfunction in mesaticephalic and brachycephalic dogs
- Assess patient-specific variables, including weight, age and skull geometry, for confounding effect on quantitative CT data in mesaticephalic and brachycephalic dogs
- Assess the effect of nasal septal deviation and caudal aberrant turbinates on CT measurements of the nasal cavity in mesaticephalic and brachycephalic dogs
- Assess the variation of nasal CT measurements between brachycephalic breeds of dogs.

B. Study 2 on histopathological sections of the nasal cavity of puppies (mesaticephalic, brachycephalic and Norwich Terriers) aimed to:

- Standardize a protocol for processing neonatal and adult intranasal epithelium
- Identify (map) the different types of epithelium lining
- Measure the relative contribution of different types of epithelium to the nasal cavity
- Describe the changes in distribution of the intranasal turbinates and compare histopathological differences in the submucosa

C. Study 3 on computational fluid dynamics simulation of intranasal flow pattern aimed to:

- Measure the wall shear stress between brachycephalic and mesaticephalic dogs; and among brachycephalic breeds
- Compare resistance and pressure drop between brachycephalic and mesaticephalic dogs and relate them to intranasal anatomical abnormalities
- Describe the flow pattern in mesaticephalic dogs and various breeds of brachycephalic dogs (BAS patients).

## **CHAPTER 2: Materials and Methods**

## **STUDY 1**

### Patient Selection

Canine patients were recruited from the Michigan State University (MSU) Veterinary Medical Center (VMC) (January 2015-January 2016) with informed owner consent and approval from the Institutional Animal Care and Use Committee (10/14-186-00). Mesaticephalic canine patients (n=9) that had no previous history of nasal disease and whose physical and clinical examination revealed no current nasal morbidity were included in the study. Mesaticephalic canine patients were chosen from the pool of dogs that were scheduled to obtain a computed tomography (CT) scan of some body part aside from the head or neck. Furthermore, only mesaticephalic dogs that weighed 25kg or less were admitted to the study, in order to control for body weight differences between mesaticephalic and brachycephalic patients. Dolichocephalic patients were excluded from the study. Recruitment for the brachycephalic group (n=15) was drawn from all brachycephalic dogs that chronologically presented to the hospital excluding emergency presentations. Many were presenting for surgical correction of brachycephalic airway syndrome abnormalities, including stenotic nares, elongated soft palate, everted tonsils, everted laryngeal sacculles, and various grades of laryngeal collapse. The breed, age, weight and skull type of each patient was recorded during physical examination.

### CT Examination and Nasal Measurements

Animals were anesthetized during CT examination and placed on sternal recumbency. The dogs were extubated and upper jaws were suspended with tape behind their incisors to allow for better visualization and reliability of obtained CT data.<sup>92,93</sup> No padding was applied

below the head and neck to avoid pressure which could potentially displace tissues in the airway. Computed tomography images were obtained using a Brightspeed 16 slice CT scanner (General Electric Healthcare, Chicago, IL) or a Revolution EVO 64 Slice CT Scanner (General Electric Healthcare, Chicago, IL) and the same parameters. Transverse sections, 0.625mm or 1.25mm thick, were acquired at 120 kVp and variable filament current (mA). Image acquisition, which lasted for less than a minute was followed by intubation for other procedures (including surgery for brachycephalic dogs), further CT acquisition as was the case with mesaticephalic dogs or allowed to recover.

CT images were uploaded to the MSU VMC Picture Archiving and Communication System (Horizon Medical Imaging, McKesson Corporation, San Francisco, CA). Standard algorithm Digital Imaging and Communications in Medicine (DICOM) images were downloaded to medical imaging processing software, Mimics 20.0 (Materialise, Leuven, Belgium).

On canine CT, the rostral border of air in the nasal cavity was where contact was made between the dorsal and ventral lateral nasal cartilages (Figure 2). The caudal border of nasal cavity was at the level of the nasopharyngeal meatus, where the hard palate transitioned to soft palate (Figure 2). However, the entire volume of air in the frontal sinus and other parts of the nasal cavity, dorsal to the nasopharyngeal meatus was included in total air volume. Using, a Hounsfield Unit threshold of -1024 to -300, total air volume, maxillary sinus volume, frontal sinus volume and cross-sectional areas was segmented. The first cross-sectional area (CSA 1), was at the level where the nasal bone and hard palate became complete, dorsally and ventrally, respectively (Figure 2). Moving caudally, the second cross-sectional area (CSA 2) was at the most caudal aspect of the choanae, shortly before the septum begins to disappear (Figure 2). The third cross-sectional area (CSA 3) was the volume of air in the

caudal aspect of the nasopharyngeal meatus, before the hard palate transitions to soft palate (Figure 2). All cross-sectional areas (CSA 1, CSA 2, CSA 3) excluded the volumes of air in the maxillary recess and frontal sinus, and were obtained by dividing their respective cross-sectional volumes by corresponding CT slice thickness. The maxillary recess and frontal sinus have shown low air-velocity and stagnant flow patterns which may suggest non-active involvement in respiration even though the maxillary recess, unlike the frontal sinus, is in free communication with the nasal cavity and involved in thermoregulation.<sup>75,94,95</sup> The functional respiratory air volume was determined by:

$$\text{Functional respiratory air volume} = \text{Total air volume} - (\text{Frontal sinus volume} + \text{Maxillary recess volume})$$

Tissue volume within the functional respiratory compartment (total air compartment excluding the maxillary recess and frontal sinus) was measured from where the lateral nasal bones first appear to where the kidney-shaped, nasal glands surrounding the vomer bone first appears (using -380 to 117) and to the nasopharyngeal meatus where the hard palate transitions to the soft palate (using -660 to 117) for consistency across mesaticephalic and brachycephalic dogs. The tissue volume within the functional respiratory compartment and functional respiratory air volume, together, comprised the functional nasal volume.

On a mid-sagittal slice, the length of the nasal cavity was measured from the tip of the nose to the choanae and sphenoid bones. In addition, the skull length and width for each dog was measured to determine their ratio, the LW index as previously described<sup>1,28,96</sup>. The presence or absence of intranasal abnormalities, including nasal septal deviation and caudal aberrant

turbinates was noted. Similar to studies on sleep apnea and for comparative anatomical analysis<sup>77</sup>, the average cross-sectional area (CSA) as determined by:

$$\text{Average CSA} = \text{Total air volume} / \text{length of the nasal cavity}$$

### Statistical Analysis

The relative volumes of the frontal sinus, maxillary recess and functional respiratory air volume were expressed as fractions of total air volume and compared between brachycephalic and mesaticephalic dogs under study using unpaired t-test or Mann-Whitney test. The functional nasal volume, made up of functional respiratory air volume and tissue volume within the functional respiratory compartment, the length of the nasal cavity, ratios of the functional nasal volume to the different cross-sectional areas (CSA 1, CSA 2, CSA 3) were also analyzed by unpaired t-test or Mann-Whitney test as appropriate. The effect the presence of septal deviation and aberrant turbinate have on the nasal cavity was analyzed by comparing nasal cavity measurements in all the dogs using unpaired t-test or Mann-Whitney test. Among brachycephalic dogs, the variation of nasal measurements with breed was analyzed using One-way ANOVA (followed by Tukey's multiple comparison for significantly different results) or Kruskal-Wallis test (followed by Dunn's test for significantly different results). The relationship between measurements in the nasal cavity and potential confounding variables, including weight and skull length-width (LW) index, was assessed using correlation and linear regression. Thereafter, skull measurements were normalized to body weight and LW index and analyzed using unpaired t-test (or Mann-Whitney test) and One-way ANOVA (or Kruskal Wallis test). All analyses were performed

using GraphPad Prism 8.0 (GraphPad Software, San Diego, CA) and statistical significance was set at  $p < 0.05$ .

## **STUDY 2**

### **Animals**

Norwich Terrier (n = 7), mesaticephalic (mixed breed of flat coated retrievers, n = 6) and brachycephalic (French Bulldog, n = 2) puppies were used to describe and compare the histologic differences of the intranasal epithelium, submucosal tissues and changes in the distribution of intranasal turbinates in neonatal (1-14 day old) dogs.

### **Histopathology**

Canine skulls from freshly (< 12hours) euthanized or dead puppies were fixed in 10% Neutral Buffered Formalin, in a volume that is 3 times the head size of the dog. Formalin will be instilled into the pharynx and both nasal cavities before placing into the container of formalin. After fixation, the mandibles were removed and the nasal cavity was decalcified in 13% formic acid, dehydrated in 70% alcohol, sectioned and paraffin embedded. The first section (T1) was obtained at the level of the incisive papilla of the hard palate. Subsequent sections, rostro-caudally, were obtained by moving a distance, the equivalent of every two ridges on the hard palate to obtain T2-T8 which extends into the soft palate at the level of the nasopharygeal meatus (See Figure 6). Each section was stained with hematoxylin and eosin.

## Nasal morphometry

Tissue sections were digitized with a slide scanner (VS 110 Olympus America, Center Valley, PA). The different types of epithelium- squamous, transitional, olfactory and respiratory- lining all the sections (T1-T8) were measured and mapped for identification, quantification and appropriate description using the same slide scanner (VS 110 Olympus America, Center Valley, PA). Comparative studies describing the various epithelial types in the nasal cavity of rats and humans are well documented.<sup>97,98</sup>

Stratified squamous epithelium is identifiable by several layers of squamous cells that become increasingly flatter toward the luminal surface of the nasal cavity. The transitional epithelium provides the continuum between squamous and respiratory epithelium and is less ciliated (or non-ciliated) cuboidal (to columnar). Olfactory epithelium is distinguishable by its pseudostratified columnar appearance. The abundance of Bowman's glands, uniform lining of sustentacular cells and nerve bundles of olfactory sensory neurons make the olfactory epithelium visually recognizable on histopathology. Lastly, the respiratory epithelium is ciliated pseudostratified cuboidal to columnar among which are variable numbers of Goblet cells and below whose lamina propria are secretory glands.

Morphometric methods were used to measure the relative contribution of the various epithelia to the nasal cavity.

## Statistical analysis

The relative contributions of the olfactory, squamous, transitional and respiratory epithelium were expressed as fractions of the total length of epithelia, and analyzed using

One-way ANOVA. All analyses were performed using GraphPad Prism 8.0 (GraphPad Software, San Diego, CA) and statistical significance was set at  $p < 0.05$ .

### **STUDY 3**

Functional Imaging (Computational Fluid Dynamics simulation)

After segmentation of high-resolution CT images, acquired three-dimensional (3-D) computer aided design (CAD) models were exported in stereolithographic (STL) format using smoothing factor of 0.9 and 5 iterations (Figure 5). The STL files were fixed in Meshmixer 3.5 (Autodesk, San Rafael, California) to fix holes which preclude CFD analysis. A pre-processing software (ICEM-CFD 19.2, Ansys, Canonsburg, PA) divided the exported 3-D model into tetrahedral meshes, typically 490,000-4,650,000. Boundary surfaces were allocated, as inlet (at the level of the nares), outlet (nasopharynx) and the wall (the nasal cavity between the nares and the nasopharynx) (Figure 5). Meshes were exported to numerical software (FLUENT 19.2, Ansys, Canonsburg, PA) for simulation. The flow was assumed to be laminar, incompressible air (having constant air density  $1.185 \text{ kg/m}^3$  and viscosity  $1.831 \times 10^{-5} \text{ kg/m/s}$ ), no slip condition, inlet gauge pressure of 0 atm (absolute pressure of 1atm) for Newtonian fluids. Simulations were run for 1000 iterations to get convergence of mass flow rate and velocities which was judged at approximately  $10^{-4}$ , as validated in previous studies.<sup>82,83,87,99</sup> The mass flow rate in mesaticephalic and brachycephalic dogs during resting conditions (laminar flow) was assumed to be 0.82 L/s and 0.28 L/s, respectively as previously reported.<sup>100</sup> Parameters of interest that were acquired from computational fluid dynamics analysis using commercial software (CFD Post, 19.2, Ansys, Canonsburg, PA) included:

- pressure drop over the upper airway ( $\Delta P = P_{\text{inlet}} - P_{\text{outlet}}$ )
- mass flow rate through the upper airway ( $\dot{m}$ )
- Resistance ( $\Delta P / \dot{m}$ )
- Intraluminal pressures and velocities at the smallest and largest cross-sectional area ( $P_{\text{min}}$ )
- Minimum velocity
- Maximum velocity
- Wall shear stress
- Velocity streamlines (field)
- Pressure contours (gradients).

#### Statistical analysis

Shear stress, intranasal airway resistance and pressure drop were analyzed using Mann-Whitney U test for comparison of brachycephalic and mesaticephalic dogs. This analysis was performed using GraphPad Prism 8.0 (GraphPad Software, San Diego, CA) and statistical significance was set at  $p < 0.05$ .

## CHAPTER 3: Results

## STUDY 1

Relevant physical features of the dogs enrolled in the study are presented in Table 4.1. Originally, 10 mesaticephalic dogs and 16 brachycephalic dogs were enrolled in the study. However, a French bulldog and a Golden retriever, both having intranasal disease conditions (including tumor) were excluded from further analyses. Mixed breeds (mesaticephalic dogs) and French bulldogs (brachycephalic dogs) were the predominant breeds in the study. The mean ages of mesaticephalic and brachycephalic dogs were 61.2 months (5.1 years) and 43.9 months (3.7 years), respectively. Brachycephalic and mesaticephalic dogs were of comparable mean weights, having 15.6kg and 14.2kg, respectively. The skull length-width (LW) index was less than 1.44 in all brachycephalic dogs but greater than or equal to 1.44 in mesaticephalic dogs.

The various compartments in the nasal cavity of mesaticephalic and brachycephalic dogs are presented in Table 4.2. Together, the frontal sinus, maxillary recess and functional respiratory air volumes constitute the total air volume (Figure 2). In mesaticephalic dogs, the frontal sinuses, maxillary recesses and functional respiratory air comprise 25%, 7% and 69% of their total air volume, respectively. Whereas in brachycephalic dogs, the frontal sinuses, maxillary recesses and functional respiratory air constitute 20%, 5% and 75% of their total air volumes. All three anatomical compartments did not significantly ( $p > 0.05$ ) differ between mesaticephalic and brachycephalic dogs.

The functional nasal volume is made up of functional respiratory air and the tissues within the functional respiratory compartment (refer to Figure 2). It is the nasal volume involved with respiration (that is, excluding frontal sinuses and maxillary recesses). Brachycephalic

dogs had higher (54%) tissue volume than mesaticephalic dogs (52%) although this difference was not significant ( $p > 0.05$ ). Conversely, mesaticephalic dogs had higher (48%) functional respiratory air than brachycephalic (46%) dogs and again, this difference was not significant ( $p > 0.05$ ). The length of the nasal cavity from the tip of the nose to the choanae or sphenoid bone was higher ( $p < 0.05$ ) in mesaticephalic dogs than in brachycephalic dogs.

To relate the anatomy of the nasal cavity with function, the functional respiratory air volume passing through cross-sectional areas (CSA 1, CSA 2, CSA 3) (refer to Figure 2) at specified landmarks was determined. Generally, more air volume had to pass through the cross-sectional areas in mesaticephalic than in brachycephalic dogs and the difference was significant ( $p < 0.05$ ) for CSA 1. The average cross-sectional area of air was not significantly different ( $p > 0.05$ ) between mesaticephalic and brachycephalic dogs.

To control for confounding effects that body weight and skull variation may bring to comparisons between mesaticephalic and brachycephalic dogs, data were normalized to body weight (BW) as well as skull length-width (LW) index as presented in Table 4.3. The frontal sinus volume, maxillary recess volume, functional respiratory air volume and tissue volume within the functional respiratory compartment were significantly ( $p < 0.05$ ) higher in mesaticephalic than in brachycephalic dogs. However, the cross-sectional areas (CSA 1, CSA 2, CSA 3) were not significantly ( $p > 0.05$ ) different between mesaticephalic and brachycephalic dogs.

To account for breed variation among brachycephalic dogs, measurements of their nasal cavities are shown in Table 4.4. The fraction of total air that the frontal sinus comprises, the length of the nasal cavity, the functional respiratory air passing through CSA 3 and the average cross-sectional areas were significantly ( $p < 0.05$ ) higher in English bulldogs

compared to pugs and French bulldogs. Remarkably, the fraction of total air that the functional respiratory air volume comprises was significantly ( $p < 0.05$ ) lower in English Bulldogs compared to pugs and French bulldogs.

Normalized data for brachycephalic dogs showing variation with breeds is presented in Table 4.5. The CSA 2 is significantly ( $p < 0.05$ ) higher in English bulldogs than in pugs but is similar to French bulldogs. However, the frontal sinus volume, maxillary recess volume, functional respiratory air volume and tissue volume within the functional respiratory compartment were higher in English bulldogs compared to French bulldogs and pugs.

The effect that anatomical abnormalities (septal deviation and/or aberrant turbinate) had on the nasal cavity is shown in Table 4.6 and Table 4.7. There was no significant ( $p > 0.05$ ) difference in terms of fraction of total air that the frontal sinus, functional respiratory air volume and maxillary recess comprise between dogs that had or did not have the abnormalities. In addition, the fraction of the functional nasal volume that the functional respiratory air and tissue volume comprise is not significantly ( $p > 0.05$ ) different among groups that had or did not have the anatomical abnormalities. However, absolute values of the maxillary recess volume, functional respiratory air volume and tissue volume within the functional respiratory compartment that were normalized to BW were significantly ( $p < 0.05$ ) higher in the absence of septal deviation and aberrant turbinate.

The association between body weight and various skull measurements are presented in Figures 1a and 1b for mesaticephalic and brachycephalic dogs, respectively. Among mesaticephalic and brachycephalic dogs, body weight was significantly ( $p < 0.05$ ) positively correlated ( $r = 0.69-0.98$ ) with CSA 3, maxillary recess volume, frontal sinus volume, functional respiratory air volume, total air volume, tissue volume within the functional

respiratory compartment, fraction of total air that the frontal sinus comprises, length of the nasal cavity (choanae and sphenoid bone), skull length, skull width and average CSA. Furthermore, strong negative correlation between body weight and fraction of total air that functional respiratory air volume comprises was observed in brachycephalic ( $r = -0.85$ ) and mesaticephalic ( $r = -0.70$ ) dogs. In mesaticephalic but not brachycephalic dogs, significant ( $p < 0.05$ ) positive correlation between body weight and the CSA 2 ( $r = 0.92$ ) and fraction of functional nasal volume that the functional respiratory air comprises ( $r = 0.86$ ) was observed. However, the fraction of functional nasal volume occupied by tissues significantly ( $p < 0.05$ ) negatively correlated ( $r = -0.86$ ) with body weight. In contrast, in only brachycephalic dogs, the functional respiratory air volume passing through CSA 3 was significantly ( $p < 0.05$ ) positively correlated ( $r = 0.60$ ) with body weight.

Age did not show any significant ( $p > 0.05$ ) association with skull measurements in brachycephalic dogs (data not shown). As shown in Figure 1c, the ratio of functional respiratory air volume to CSA 1, negatively correlated ( $r = -0.69$ ) significantly ( $p < 0.05$ ) with age in mesaticephalic dogs. Other skull measurements in mesaticephalic dogs did not show any significant ( $p > 0.05$ ) association with age (data not shown).

The relationship between the skull length-width index and measurements in the nasal cavity was assessed as shown in Figure 1d for mesaticephalic dogs. Length-width index significantly ( $p < 0.05$ ) positively correlated ( $r = 0.67-0.86$ ) with the total air volume, maxillary recess volume, frontal sinus volume, functional respiratory air volume, tissue volume within the functional respiratory compartment, ratio of the functional respiratory air volume to functional nasal volume, length of the nasal cavity, ratio of the functional respiratory air volume to CSA 3 and ratio of the functional respiratory air volume to CSA 2.

However, the ratio of tissue volume within the functional respiratory compartment to functional nasal volume significantly ( $p < 0.05$ ) negatively correlated ( $r = -0.67$ ) with length-width index. In brachycephalic dogs, the skull length-width index did not significantly ( $p > 0.05$ ) correlate with intranasal measurements (data not shown).

## **STUDY 2**

Morphometric data showing the histologic distribution of the different types of epithelium in Norwich Terrier puppies, mesaticephalic and brachycephalic puppies are shown in Table 4.8. Mesaticephalic puppies had more (36%) olfactory epithelial covering than brachycephalic (French Bulldogs) (31%) and Norwich Terrier (32%) puppies. The intranasal epithelial contribution made by squamous epithelium (4-7%), transitional epithelium (2-7%) and respiratory epithelium (57-58%) was similar between Norwich Terrier, mesaticephalic and brachycephalic puppies. Interestingly, the fraction of the total respiratory epithelium formed by the lining of the choanae and nasopharyngeal meatus was similar in Norwich Terriers and mesaticephalic puppies (both 24%) but more in brachycephalic puppies (33%). Overall, there was no statistical ( $p > 0.05$ ) difference between epithelial types for Norwich Terriers, mesaticephalic and brachycephalic puppies.

## **STUDY 3**

Shear stress, intranasal airway resistance and pressure drop were generally higher in brachycephalic dogs than in mesaticephalic dogs, although statistical significance was only observed with intranasal airway resistance as shown in Table 4.9.

## **APPENDIX**

**Table 4.1: Characteristics of dogs enrolled in the study.**

Dog type and breed (number)	Mean age (months) (range)	Mean body weight (kg) (range)	Mean skull length (mm) (range)	Mean skull width (mm) (range)	Mean skull length/ width (range)
Mesaticephalic (9)	61.2 (9.0-144.0)	14.2 (4.5-28.5)	150.9 (106.0-203.0)	93.9 (69.0-116.0)	1.6 (1.4-1.8)
Mixed breeds (5)					
German Shorthaired Pointer (1)					
Miniature Pinscher (1)					
Brittany Spaniel (1)					
Labradoodle (1)					
Brachycephalic (15)	43.9 (5.0-120.0)	15.6 (8.2-29.1)	105.5 (86.0-134.0)	108.4 (91.0-133.0)	1.0 (0.8-1.1)
English bulldog (4)					
French bulldog (8)					
Pug (2)					
Boston terrier (1)					

**Table 4.2: Comparison of the nasal cavity of mesaticephalic and brachycephalic of dogs.**

	Mean <sup>#</sup> ± SD
Fraction <sup>†</sup> frontal sinus volume comprises	
Mesaticephalic	0.25 ± 0.12 <sup>a</sup>
Brachycephalic	0.20 ± 0.17 <sup>a</sup>
Fraction maxillary recess comprises	
Mesaticephalic	0.07 ± 0.03 <sup>a</sup>
Brachycephalic	0.05 ± 0.02 <sup>a</sup>
Fraction functional respiratory air volume comprises	
Mesaticephalic	0.69 ± 0.10 <sup>a</sup>
Brachycephalic	0.75 ± 0.17 <sup>a</sup>
Functional respiratory air/ Functional nasal volume <sup>λ</sup>	
Mesaticephalic	0.48 ± 0.13 <sup>a</sup>
Brachycephalic	0.46 ± 0.09 <sup>a</sup>
Tissue volume within the functional respiratory compartment/ Functional nasal volume	
Mesaticephalic	0.52 ± 0.13 <sup>a</sup>
Brachycephalic	0.54 ± 0.09 <sup>a</sup>
Length of the nasal cavity (Choanae)	
Mesaticephalic	84.34 ± 20.81 <sup>a</sup>
Brachycephalic	53.72 ± 7.37 <sup>b</sup>
Length of the nasal cavity (Sphenoid bone)	
Mesaticephalic	107.80 ± 27.51 <sup>a</sup>
Brachycephalic	62.38 ± 11.57 <sup>b</sup>
Functional respiratory air/ CSA* 1	
Mesaticephalic	154.60 ± 73.86 <sup>a</sup>
Brachycephalic	66.12 ± 32.27 <sup>b</sup>
Functional respiratory air/ CSA 2	
Mesaticephalic	44.05 ± 15.27 <sup>a</sup>
Brachycephalic	35.68 ± 15.18 <sup>a</sup>
Functional respiratory air/ CSA 3	
Mesaticephalic	196.70 ± 109.90 <sup>a</sup>
Brachycephalic	108.10 ± 39.03 <sup>a</sup>
Average CSA	
Mesaticephalic	274.20 ± 178.90 <sup>a</sup>
Brachycephalic	225.00 ± 121.00 <sup>a</sup>

<sup>a, b</sup> Unmatched superscripts indicate significant (p<0.05) difference in the column for each set of variables

<sup>#</sup>Number of Mesaticephalic dogs = 9, Brachycephalic dogs = 15

\*Cross-Sectional Area

<sup>†</sup>Total air volume is the sum of frontal sinus, maxillary recess and functional respiratory air; each was expressed as a fraction of total air; and can be expressed as percentages (%) by multiplying by 100

<sup>λ</sup>Functional nasal volume is the sum of functional respiratory air and tissue volume therein; and can be expressed as percentages (%) by multiplying by 100

**Table 4.3: Comparison of nasal cavity statistic in mesaticephalic and brachycephalic dogs after normalizing to skull length-width (LW) index and body weight (BW)**

	Mean# ± SD (LW)	Mean# ± SD (BW)
CSA* 1		
Mesaticephalic	157.10 ± 215.70 <sup>a</sup>	14.14 ± 13.78 <sup>a</sup>
Brachycephalic	228.80 ± 147.20 <sup>a</sup>	16.56 ± 10.95 <sup>a</sup>
CSA 2		
Mesaticephalic	359.80 ± 244.10 <sup>a</sup>	37.87 ± 13.85 <sup>a</sup>
Brachycephalic	381.10 ± 195.20 <sup>a</sup>	26.96 ± 15.14 <sup>a</sup>
CSA 3		
Mesaticephalic	91.58 ± 96.49 <sup>a</sup>	9.45 ± 5.49 <sup>a</sup>
Brachycephalic	114.60 ± 40.11 <sup>a</sup>	8.24 ± 3.58 <sup>a</sup>
Total air volume		
Mesaticephalic	24782.00 ± 19134.00 <sup>a</sup>	2400.00 ± 1148.00 <sup>a</sup>
Brachycephalic	20230.00 ± 18292.00 <sup>a</sup>	1180.00 ± 610.00 <sup>b</sup>
Frontal sinus volume		
Mesaticephalic	7708.00 ± 6692.00 <sup>a</sup>	696.70 ± 499.60 <sup>a</sup>
Brachycephalic	6389.00 ± 9400.00 <sup>a</sup>	289.40 ± 343.40 <sup>b</sup>
Maxillary recess volume		
Mesaticephalic	1278.00 ± 934.80 <sup>a</sup>	135.60 ± 51.94 <sup>a</sup>
Brachycephalic	823.70 ± 553.40 <sup>a</sup>	52.79 ± 24.85 <sup>b</sup>
Functional respiratory air volume		
Mesaticephalic	15796.00 ± 11697.00 <sup>a</sup>	1567.00 ± 631.10 <sup>a</sup>
Brachycephalic	13018.00 ± 8736.00 <sup>a</sup>	838.20 ± 349.10 <sup>b</sup>
Tissue volume within the functional respiratory compartment		
Mesaticephalic	13329.00 ± 6974.00 <sup>a</sup>	1575.60 ± 297.30 <sup>a</sup>
Brachycephalic	14078.00 ± 6835.00 <sup>a</sup>	931.50 ± 280.00 <sup>b</sup>

<sup>a, b</sup> Unmatched superscripts indicate significant (p<0.05) difference in the column for each set of variables

#Number of Mesaticephalic dogs = 9, Brachycephalic dogs = 15

\*Cross-Sectional Area

**Table 4.4: Variation of the nasal cavity among enrolled brachycephalic breeds.**

	Mean <sup>#</sup> ± SD
Fraction <sup>†</sup> frontal sinus volume comprises	
French bulldogs	0.14 ± 0.12 <sup>a</sup>
English bulldogs	0.43 ± 0.06 <sup>b</sup>
Pugs	0.06 ± 0.05 <sup>a</sup>
Fraction maxillary recess comprises	
French bulldogs	0.05 ± 0.01 <sup>a</sup>
English bulldogs	0.04 ± 0.02 <sup>a</sup>
Pugs	0.04 ± 0.02 <sup>a</sup>
Fraction functional respiratory air volume comprises	
French bulldogs	0.81 ± 0.12 <sup>a</sup>
English bulldogs	0.53 ± 0.07 <sup>b</sup>
Pugs	0.90 ± 0.03 <sup>a</sup>
Functional respiratory air/ Functional nasal volume <sup>λ</sup>	
French bulldogs	0.45 ± 0.09 <sup>a</sup>
English bulldogs	0.49 ± 0.13 <sup>a</sup>
Pugs	0.42 ± 0.05 <sup>a</sup>
Tissue volume within the functional respiratory compartment/ Functional nasal volume	
French bulldogs	0.54 ± 0.09 <sup>a</sup>
English bulldogs	0.51 ± 0.13 <sup>a</sup>
Pugs	0.58 ± 0.05 <sup>a</sup>
Length of the nasal cavity (Choanae)	
French bulldogs	49.19 ± 3.23 <sup>a</sup>
English bulldogs	64.82 ± 1.49 <sup>b</sup>
Pugs	51.32 ± 0.23 <sup>a</sup>
Length of the nasal cavity (Sphenoid bone)	
French bulldogs	54.52 ± 3.25 <sup>a</sup>
English bulldogs	79.85 ± 4.33 <sup>b</sup>
Pugs	60.50 ± 3.56 <sup>a</sup>
Functional respiratory air/ CSA* 1	
French bulldogs	51.43 ± 23.52 <sup>a</sup>
English bulldogs	83.62 ± 27.28 <sup>a</sup>
Pugs	102.30 ± 47.86 <sup>a</sup>
Functional respiratory air/ CSA 2	
French bulldogs	31.70 ± 15.16 <sup>a</sup>
English bulldogs	42.66 ± 13.54 <sup>a</sup>
Pugs	42.97 ± 22.87 <sup>a</sup>
Functional respiratory air/ CSA 3	
French bulldogs	88.64 ± 27.48 <sup>a</sup>
English bulldogs	154.70 ± 30.80 <sup>b</sup>
Pugs	83.96 ± 2.93 <sup>a</sup>
Average CSA	
French bulldogs	189.70 ± 55.19 <sup>a</sup>
English bulldogs	368.40 ± 143.30 <sup>b</sup>
Pugs	123.70 ± 35.64 <sup>a</sup>

<sup>a, b</sup> Unmatched superscripts indicate significant ( $p < 0.05$ ) difference in the column for each set of variables

<sup>#</sup>Number of French bulldogs = 8, English bulldog = 4, Pugs = 2; only brachycephalic breeds having  $n > 1$  were used in this analysis.

\*Cross-Sectional Area

<sup>†</sup>Total air volume is the sum of frontal sinus, maxillary recess and functional respiratory air; each was expressed as a fraction of total air; and can be expressed as percentages (%) by multiplying by 100

<sup>λ</sup>Functional nasal volume is the sum of functional respiratory air and tissue volume therein; and can be expressed as percentages (%) by multiplying by 100

**Table 4.5: Comparison of nasal cavity statistic among enrolled brachycephalic breeds after controlling for skull length-width (LW) index and body weight (BW)**

	Mean <sup>#</sup> ± SD (LW)	Mean <sup>#</sup> ± SD (BW)
CSA* 1		
French bulldogs	223.30 ± 104.50 <sup>a</sup>	21.47 ± 11.77 <sup>a</sup>
English bulldogs	334.60 ± 205.50 <sup>a</sup>	12.16 ± 6.76 <sup>a</sup>
Pugs	75.76 ± 53.36 <sup>a</sup>	4.54 ± 2.44 <sup>a</sup>
CSA 2		
French bulldogs	352.50 ± 157.10 <sup>ab</sup>	32.81 ± 16.85 <sup>a</sup>
English bulldogs	572.80 ± 180.10 <sup>a</sup>	22.07 ± 9.92 <sup>a</sup>
Pugs	188.70 ± 143.10 <sup>b</sup>	11.24 ± 6.74 <sup>a</sup>
CSA 3		
French bulldogs	112.40 ± 19.48 <sup>ab</sup>	10.59 ± 3.25 <sup>a</sup>
English bulldogs	153.80 ± 46.43 <sup>a</sup>	5.76 ± 1.73 <sup>b</sup>
Pugs	76.77 ± 19.15 <sup>b</sup>	4.83 ± 0.22 <sup>ab</sup>
Total air volume		
French bulldogs	12551.00 ± 4532.00 <sup>a</sup>	1145.00 ± 467.80 <sup>ab</sup>
English bulldogs	45427.00 ± 18326.00 <sup>b</sup>	1703.00 ± 683.50 <sup>b</sup>
Pugs	7237.00 ± 2311.00 <sup>a</sup>	452.10 ± 53.42 <sup>a</sup>
Frontal sinus volume		
French bulldogs	2126.00 ± 2348.00 <sup>a</sup>	169.10 ± 169.90 <sup>a</sup>
English bulldogs	19437.00 ± 9355.00 <sup>b</sup>	729.00 ± 340.30 <sup>b</sup>
Pugs	460.50 ± 508.40 <sup>a</sup>	26.37 ± 26.74 <sup>a</sup>
Maxillary recess volume		
French bulldogs	630.00 ± 173.70 <sup>a</sup>	59.43 ± 25.17 <sup>a</sup>
English bulldogs	1611.00 ± 386.10 <sup>b</sup>	61.11 ± 17.80 <sup>a</sup>
Pugs	303.50 ± 30.52 <sup>a</sup>	19.80 ± 5.99 <sup>a</sup>
Functional respiratory air volume		
French bulldogs	9795.00 ± 2833.00 <sup>a</sup>	916.20 ± 350.60 <sup>a</sup>
English bulldogs	24379.00 ± 9671.00 <sup>b</sup>	912.90 ± 363.50 <sup>a</sup>
Pugs	6474.00 ± 1833.00 <sup>a</sup>	406.00 ± 32.67 <sup>a</sup>
Tissue volume within the functional respiratory compartment		
French bulldogs	11545.00 ± 2365.00 <sup>a</sup>	1051.00 ± 221.10 <sup>a</sup>
English bulldogs	23679.00 ± 5217.00 <sup>b</sup>	911.40 ± 337.50 <sup>a</sup>
Pugs	8746.00 ± 602.00 <sup>a</sup>	560.90 ± 76.92 <sup>a</sup>

<sup>a, b</sup> Unmatched superscripts indicate significant ( $p < 0.05$ ) difference in the column for each set of variables

<sup>#</sup>Number of French bulldogs = 8, English bulldog = 4, Pugs = 2; only brachycephalic breeds having  $n > 1$  were used in this analysis.

\*Cross-Sectional Area

**Table 4.6: Effect the presence of septal deviation and aberrant turbinate have on the nasal cavity**

	Mean <sup>#</sup> ± SD
Fraction <sup>†</sup> frontal sinus volume comprises	
Presence of septal deviation and/or aberrant turbinate	0.22 ± 0.18 <sup>a</sup>
Absence of both septal deviation and aberrant turbinate	0.21 ± 0.13 <sup>a</sup>
Fraction maxillary recess comprises	
Presence of septal deviation and/or aberrant turbinate	0.05 ± 0.02 <sup>a</sup>
Absence of both septal deviation and aberrant turbinate	0.06 ± 0.03 <sup>a</sup>
Fraction functional respiratory air volume comprises	
Presence of septal deviation and/or aberrant turbinate	0.73 ± 0.17 <sup>a</sup>
Absence of both septal deviation and aberrant turbinate	0.72 ± 0.12 <sup>a</sup>
Functional respiratory air/ Functional nasal volume <sup>λ</sup>	
Presence of septal deviation and/or aberrant turbinate	0.47 ± 0.09 <sup>a</sup>
Absence of both septal deviation and aberrant turbinate	0.47 ± 0.12 <sup>a</sup>
Tissue volume within the functional respiratory compartment/ Functional nasal volume	
Presence of septal deviation and/or aberrant turbinate	0.53 ± 0.09 <sup>a</sup>
Absence of both septal deviation and aberrant turbinate	0.53 ± 0.12 <sup>a</sup>
Functional respiratory air/ CSA* 1	
Presence of septal deviation and/or aberrant turbinate	71.32 ± 31.49 <sup>a</sup>
Absence of both septal deviation and aberrant turbinate	132.40 ± 82.54 <sup>a</sup>
Functional respiratory air/ CSA 2	
Presence of septal deviation and/or aberrant turbinate	36.68 ± 16.10 <sup>a</sup>
Absence of both septal deviation and aberrant turbinate	41.35 ± 14.98 <sup>a</sup>
Functional respiratory air/ CSA 3	
Presence of septal deviation and/or aberrant turbinate	114.80 ± 36.76 <sup>a</sup>
Absence of both septal deviation and aberrant turbinate	172.60 ± 112.30 <sup>a</sup>
Average CSA	
Presence of septal deviation and/or aberrant turbinate	236.40 ± 125.30 <sup>a</sup>
Absence of both septal deviation and aberrant turbinate	251.80 ± 168.80 <sup>a</sup>

<sup>a, b</sup> Unmatched superscripts indicate significant ( $p < 0.05$ ) difference in the column for each set of variables

<sup>#</sup>Number having septal deviation and/or aberrant turbinate = 13, Absence of both septal deviation and aberrant turbinate = 11

\*Cross-Sectional Area

<sup>†</sup>Total air volume is the sum of frontal sinus, maxillary recess and functional respiratory air; each was expressed as a fraction of total air; and can be expressed as percentages (%) by multiplying by 100

<sup>λ</sup>Functional nasal volume is the sum of functional respiratory air and tissue volume therein; and can be expressed as percentages (%) by multiplying by 100

**Table 4.7: Effect the presence of septal deviation and aberrant turbinate have on the nasal cavity after controlling for skull length-width (LW) index and body weight (BW)**

	Mean# ± SD (LW)	Mean# ± SD (BW)
CSA* 1		
Presence	227.10 ± 157.50 <sup>a</sup>	15.41 ± 11.19 <sup>a</sup>
Absence	172.20 ± 197.20 <sup>a</sup>	15.93 ± 13.13 <sup>a</sup>
CSA 2		
Presence	397.80 ± 200.00 <sup>a</sup>	26.70 ± 15.55 <sup>a</sup>
Absence	346.70 ± 227.50 <sup>a</sup>	36.20 ± 14.06 <sup>a</sup>
CSA 3		
Presence	113.40 ± 42.99 <sup>a</sup>	7.63 ± 3.43 <sup>a</sup>
Absence	97.17 ± 87.31 <sup>a</sup>	9.56 ± 5.05 <sup>a</sup>
Total air volume		
Presence	21961.00 ± 19095.00 <sup>a</sup>	1224.00 ± 638.10 <sup>a</sup>
Absence	21909.00 ± 18314.00 <sup>a</sup>	2126.00 ± 1200.00 <sup>a</sup>
Frontal sinus volume		
Presence	7291.00 ± 9822.00 <sup>a</sup>	325.70 ± 356.10 <sup>a</sup>
Absence	6403.00 ± 6654.00 <sup>a</sup>	579.70 ± 517.20 <sup>a</sup>
Maxillary recess volume		
Presence	885.60 ± 569.40 <sup>a</sup>	54.43 ± 23.10 <sup>a</sup>
Absence	1122.00 ± 906.40 <sup>a</sup>	118.60 ± 60.07 <sup>b</sup>
Functional respiratory air volume		
Presence	13785.00 ± 9104.00 <sup>a</sup>	844.00 ± 359.70 <sup>a</sup>
Absence	14384.00 ± 10998.00 <sup>a</sup>	1428.00 ± 655.50 <sup>b</sup>
Tissue volume within the functional respiratory compartment		
Presence	14623.00 ± 7207.00 <sup>a</sup>	912.60 ± 296.00 <sup>a</sup>
Absence	12820.00 ± 6353.00 <sup>a</sup>	1480.00 ± 340.60 <sup>b</sup>

<sup>a, b</sup> Unmatched superscripts indicate significant ( $p < 0.05$ ) difference in the column for each set of variables

#Number of Mesaticephalic dogs = 9, Brachycephalic dogs = 15

\*Cross-Sectional Area

**Table 4.8: Distribution of the types of epithelium in the nasal cavity of puppies by histomorphometry.**

	Mean# ± SD
Fraction* comprised of olfactory epithelium	
Norwich Terrier puppies	0.32 ± 0.06 <sup>a</sup>
Brachycephalic puppies	0.31 ± 0.07 <sup>a</sup>
Mesaticephalic puppies	0.36 ± 0.06 <sup>a</sup>
Fraction comprised of squamous epithelium	
Norwich Terrier puppies	0.07 ± 0.03 <sup>a</sup>
Brachycephalic puppies	0.05 ± 0.03 <sup>a</sup>
Mesaticephalic puppies	0.04 ± 0.02 <sup>a</sup>
Fraction comprised of transitional epithelium	
Norwich Terrier puppies	0.04 ± 0.02 <sup>a</sup>
Brachycephalic puppies	0.07 ± 0.07 <sup>a</sup>
Mesaticephalic puppies	0.02 ± 0.03 <sup>a</sup>
Fraction comprised of respiratory epithelium	
Norwich Terrier puppies	0.57 ± 0.04 <sup>a</sup>
Brachycephalic puppies	0.57 ± 0.02 <sup>a</sup>
Mesaticephalic puppies	0.58 ± 0.05 <sup>a</sup>
Fraction of the total respiratory epithelium formed by the lining of the choanae and nasopharyngeal meatus	
Norwich Terrier puppies	0.24 ± 0.05 <sup>a</sup>
Brachycephalic puppies	0.33 ± 0.00 <sup>a</sup>
Mesaticephalic puppies	0.24 ± 0.06 <sup>a</sup>

<sup>a, b</sup> Unmatched superscripts indicate significant ( $p < 0.05$ ) difference in the column for each set of variables

#Number of Norwich Terrier puppies = 7, brachycephalic (French bulldogs) puppies = 2, mesaticephalic puppies = 6

\*Fractions are ratios of the length of a specific epithelial type to the sum of the lengths of all epithelia in the nasal cavity and can be expressed as percentages (%) by multiplying by 100

**Table 4.9: Comparison between wall shear stress, airway resistance and pressure drop in the nasal cavities of brachycephalic and mesaticephalic dogs.**

	Mean <sup>#</sup> ± SD
Shear stress (Pa)	
Mesaticephalic dogs	52.57 ± 30.75 <sup>a</sup>
Brachycephalic dogs	155.30 ± 128.10 <sup>a</sup>
Intranasal airway resistance (1/ms)	
Mesaticephalic dogs	4472886.00 ± 5260859.00 <sup>a</sup>
Brachycephalic dogs	78494655.00 ± 85968769.00 <sup>b</sup>
Intranasal pressure drop (Pa)	
Mesaticephalic dogs	4495.00 ± 5287.00 <sup>a</sup>
Brachycephalic dogs	26924.00 ± 29487.00 <sup>a</sup>

<sup>a, b</sup> Unmatched superscripts indicate significant (p<0.05) difference in the column for each set of variables

<sup>#</sup>Number of Mesaticephalic dogs = 4, Brachycephalic dogs = 6

**Figure 1a:** Relationship between body weight and measurements in the nasal cavity of mesaticephalic dogs.

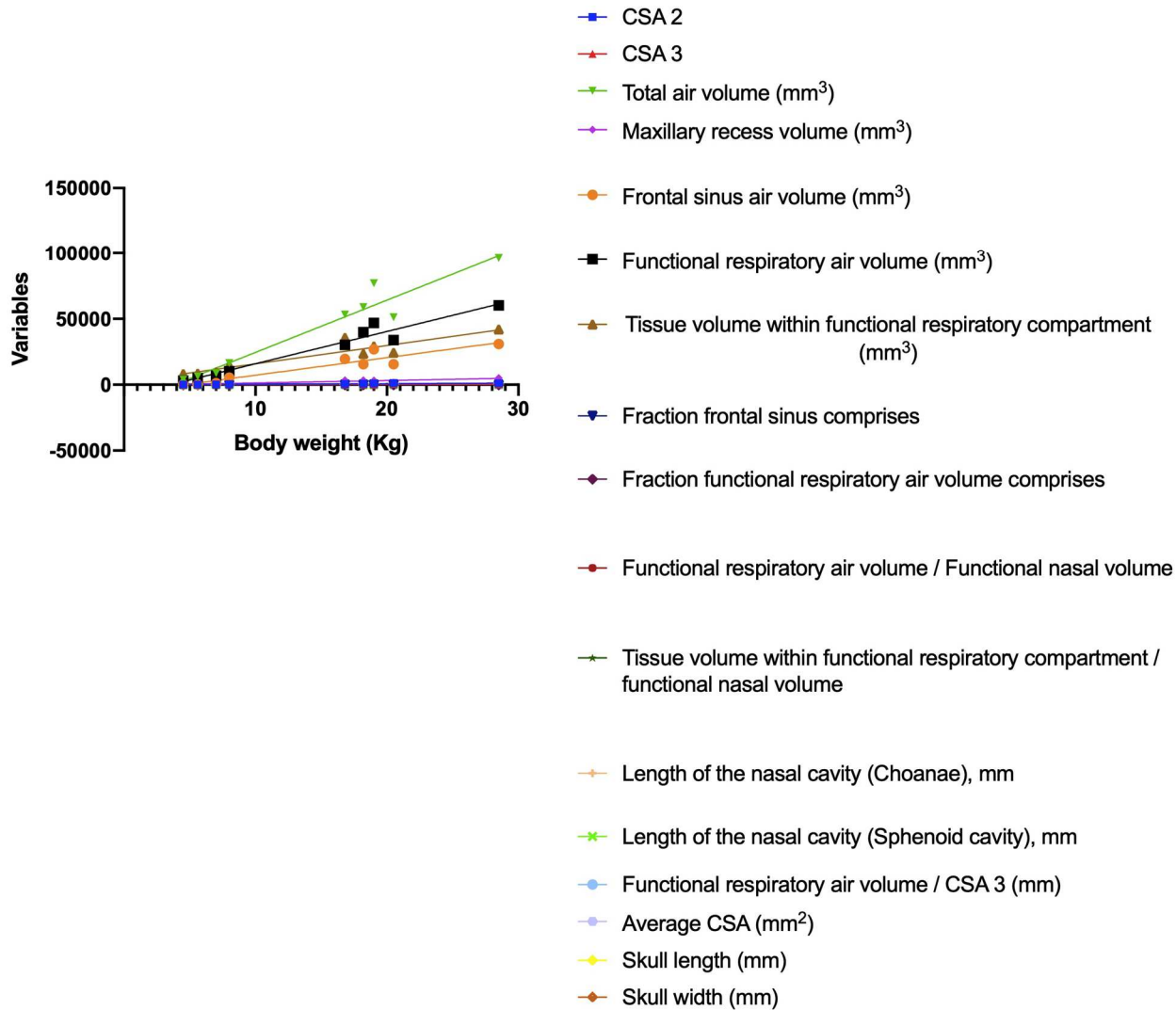


**Figure 1b:** Relationship between body weight and measurements in the nasal cavity of brachycephalic dogs.

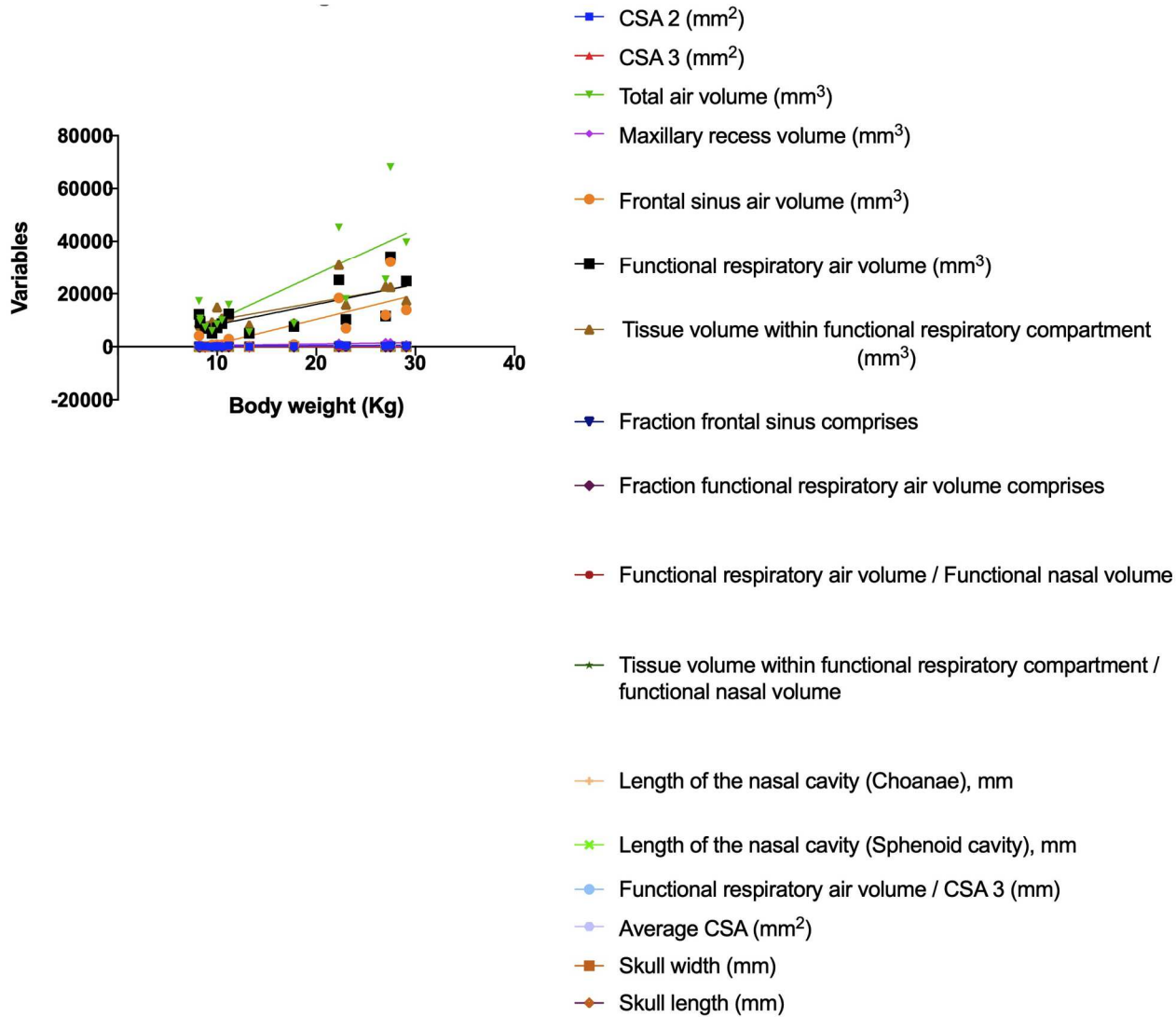
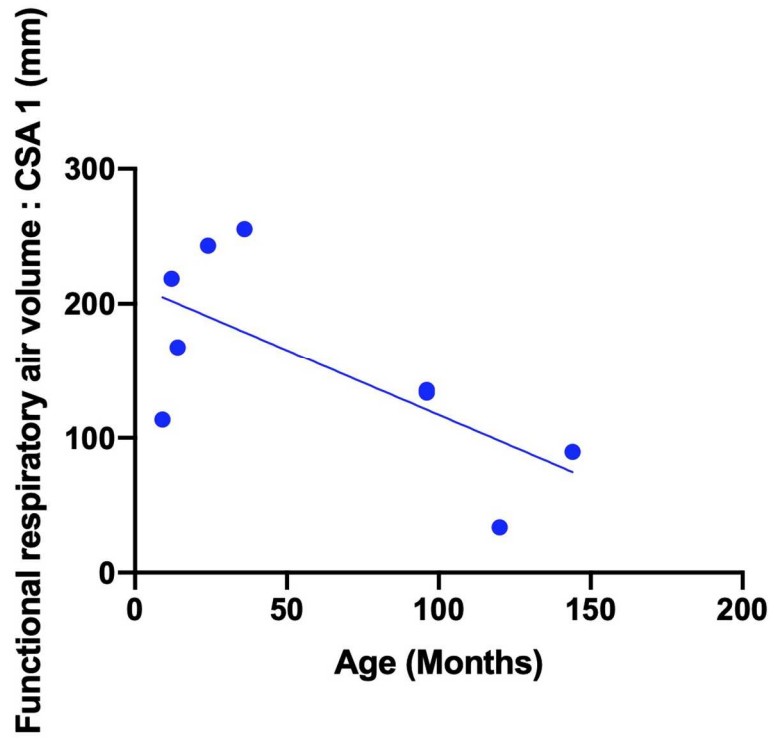
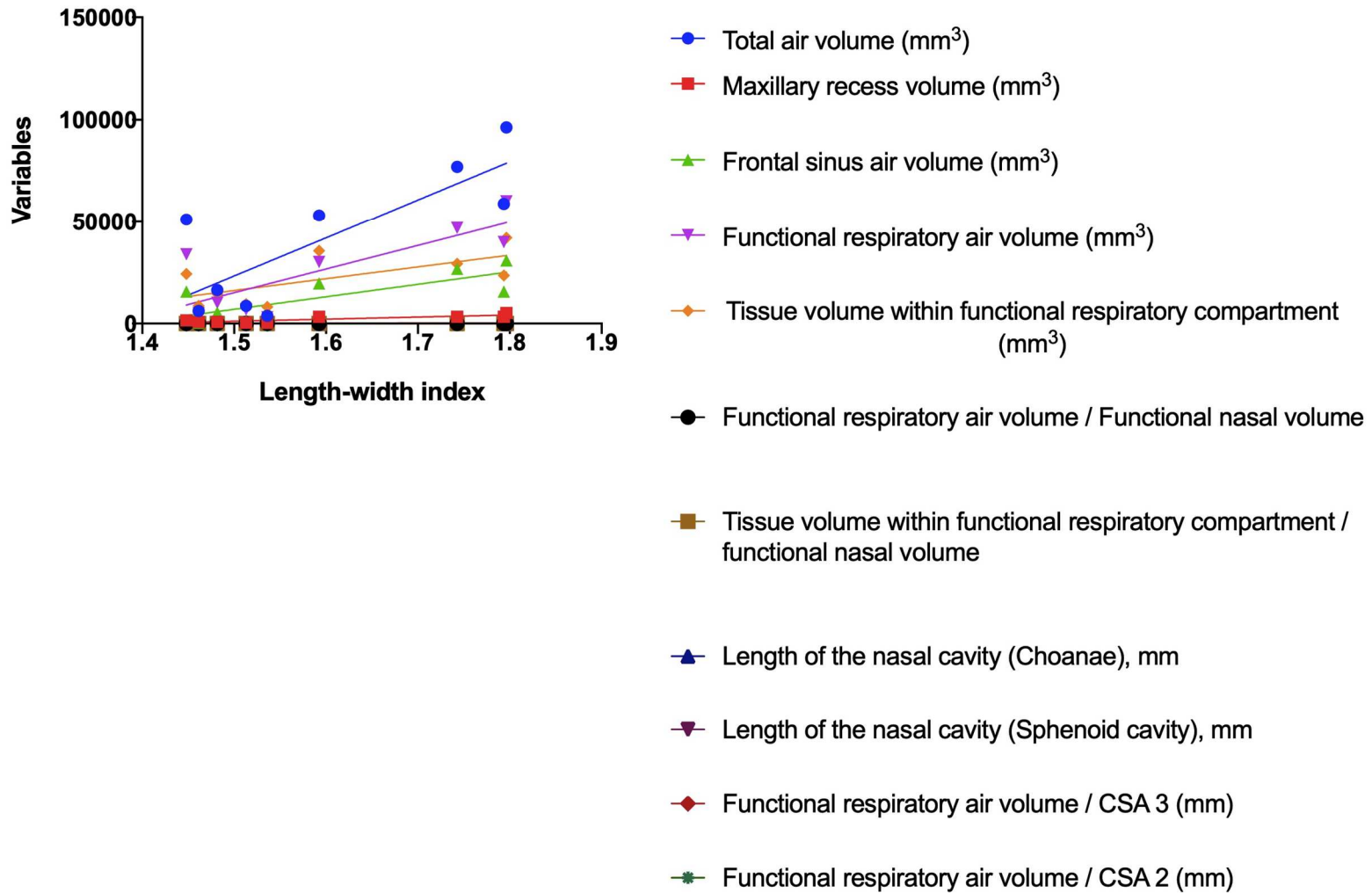


Figure 1c: Relationship between age and measurements in the nasal cavity of mesaticephalic dogs.



**Figure 1d:** Relationship between length-width index and measurements in the nasal cavity of mesaticephalic dogs



## **CHAPTER 4: Discussion and Conclusion**

## STUDY 1

The anatomy of the nasal cavity in dogs was divided into three compartments- frontal sinus, maxillary recess and functional respiratory air volumes- to effectively relate structure with function (Figure 2). Hitherto, the radiographic anatomy of the frontal sinus in brachycephalic and mesaticephalic dogs; and among brachycephalic dogs have not been compared. As macrosmatic animals, the frontal sinus functions in olfaction and is anatomically distinguishable from the nasal cavity in mesaticephalic dogs, where it constitutes part of the peripheral olfactory apparatus<sup>94,101</sup>. Among brachycephalic dogs, the frontal sinus is visually delineated on CT scans in the English bulldog but may be almost absent in some French bulldogs and pugs. Together with the maxillary recess, the frontal sinus has been suspected to exhibit stagnant air flow during sniffing in mesaticephalic dogs.<sup>75</sup> Furthermore, the maxillary recess functions in thermoregulation because of its association with the lateral nasal glands. The lateral nasal glands synthesize watery secretions which, together with tears from the nasolacrimal duct, moisten the nasal vestibule of dogs aiding in heat loss by evaporation since dogs do not have sweat glands.<sup>95</sup>

To effectively contrast stagnant air in the nasal cavity (frontal sinus and maxillary recess), this study designated dynamic air that is involved in respiration as “functional” respiratory air volume. Measured air volumes are made on CT scans of the nasal cavity and hence are not “physiologic” volumes as obtained during the likes of pulmonary function tests.

The functional respiratory air volume, together with the tissue therein, constituted the functional nasal volume (Figure 2). The higher percentage of functional nasal volume that was occupied by tissues in brachycephalic dogs, relative to mesaticephalic dogs, provides novel and specific evidence to the intranasal contribution to BAS. In addition to their bigger

geometry and total air volume, mesaticephalic dogs had higher percentage of functional respiratory air, giving them a unique advantage at respiration.

The study shows that measuring functional respiratory air volume to cross sectional area (CSA) ratio on CT is a valuable preoperative assessment index, as it provides a relationship between structure and function. Higher indices of this ratio, as reflected in the results for mesaticephalic dogs, imply superior intranasal air circulation. Therefore intranasal surgeries, should aim to improve the functional respiratory air volume to cross sectional area indices. Our choice of the three anatomical levels to measure CSA was informed by their relevance as surgical targets to improve air flow. The CSA 1 (Figure 2) was at the level where the hard palate and nasal bone, ventrally and dorsally, respectively, became fully visible on CT. This region is filled with tortuous turbinates in both mesaticephalic and brachycephalic dogs that could impede effective air flow. The CSA 2 (Figure 2), at the caudal aspect of the choanae before the nasal septum begins to disappear is an anatomical location where caudal aberrant turbinates are frequently found.<sup>13,14</sup> The nasopharyngeal meatus (CSA 3), at the transition of the hard palate to the soft palate, opens into the nasopharynx and leads directly to the lower respiratory tract (Figure 2). Therefore, potential nasal obstructions that compromise the airway at CSA 1, CSA 2, CSA 3 are important.

Correlation and regression analysis revealed a strong relationship between preoperative nasal indices obtained from CT and skull morphometry (length and width) and body weight. To control for potential confounding effects, body weight and skull morphometry may cause, we separately normalized our data to body weight and length-width index. Tidal volume as well as peak inspiratory volumes have been previously normalized to body weight to effectively assess function.<sup>70,102</sup> Among English bulldogs (brachycephalic dogs) without BAS,

body weight did not affect the degree of protrusion of the caudal aberrant turbinates.<sup>33</sup> Age did not show any association with CT measurements, except in mesaticephalic dogs, where it negatively correlated with the ratio of functional respiratory air volume to CSA. In humans, specifically men, upper airway resistance was correlated with body weight and age.<sup>39,103</sup>

Among brachycephalic breeds of dogs in this study, English bulldogs had significantly higher volume measurements of their frontal sinus, maxillary recess, functional respiratory air passing through the nasopharynx, functional respiratory air volume and average CSA than in pugs and French bulldogs. However, the cases of BAS encountered in clinical settings, in our experience, are more severe than BAS in French bulldogs and pugs. This may be explained by the fact that the fraction of total air which the functional respiratory air volume comprises is lower in English bulldogs but higher in French bulldogs and pugs. Again, our data revealed that tissue volume present within the functional respiratory air compartment was higher in English bulldogs than in pugs and French bulldogs. This provides novel insight lacking in current literature, explaining the severity in the clinical presentation of English bulldogs over pugs and French bulldogs. In addition, preoperative assessment of CT images of the brachycephalic heads, should focus on these distinguishing indices, namely fraction of total air which the functional respiratory air volume comprises and tissue volume present within the functional respiratory air compartment.

Our study showed that the maxillary sinus volume was higher in dogs that did not have nasal septal deviation and caudal aberrant turbinates. It was interesting to note that, as body weight increased, the fraction of total air which the functional respiratory air volume constituted decreased. Epidemiological studies have shown that obesity is a risk factor for upper airway disease among brachycephalic dogs and that tidal volume per body weight

significantly decreased while respiratory rate increases in obese dogs.<sup>102,104</sup> It has been suggested that obesity may mediate compromised expiration, only during hyperpnea<sup>105</sup>; and in obese brachycephalic dogs, the ratio of expiratory time to inspiratory time decreases.<sup>70</sup> This provides evidence that the upper airway disorder associated with obesity in dogs is related, at least in part, to intranasal anatomical abnormalities that affect function, specifically in terms of decreased fraction of total air which the functional respiratory air volume constitutes.

## **STUDY 2**

Our findings revealed that olfactory (31-36%), squamous (4-7%), transitional (2-7%) and respiratory epithelium (57-58%) comprised the different types of epithelium in the nasal cavity of the puppies- French bulldogs (brachycephalic), mixed breed of flat coated retrievers (mesaticephalic) and Norwich Terriers- studied. The relative contribution of the types of epithelium were similar between the various dog breeds. However, mesaticephalic and brachycephalic dogs had the most olfactory and transitional epithelia, respectively. The transitional epithelium, together with the respiratory epithelium, have implicated to be particularly susceptible to toxic insult in primates.<sup>106,107</sup> In rats, approximately 50% of their nasal cavity is lined by olfactory epithelium whereas in humans is only 3%.<sup>97,98,108,109</sup> The squamous epithelium of rats, comprise only 3.5% of their entire nasal cavity.<sup>97</sup>

The most rostral part (T1) of the nasal cavity in the puppies, the nasal vestibule, is lined by stratified squamous epithelium (Figure 3). Hair follicles were absent in all puppies' nasal vestibule. The thickness of the squamous epithelium was variable (29.18-108.70  $\mu\text{m}$ ) in puppies and made of basal cells which become horizontally flattened and keratinized

towards the airway lumen. Of the 8 sections (T1-T8, rostral-caudally), T1 was usually mostly squamous epithelium, whereas T2 was a combination of squamous epithelium lining the ventrolateral aspect (floor) and transitional epithelium lining the dorsolateral aspect of the nasal vestibule (Figure 3). Characteristically, transitional epithelium was cuboidal (4-5 cell thick) and mostly nonciliated in all puppies, with numerous surface cells that delineated them. In monkeys (primates), the transitional epithelium is histologically similar, being 4-5 cells thick.<sup>110</sup> In contrast, mice have thin (1-2 cells thick) transitional epithelium.<sup>98</sup> Electron microscopy of the transitional epithelium in mice revealed that they have increased numbers of smooth endoplasmic reticulum which functions in metabolizing xenobiotics and an abundance of microvilli that facilitate mucociliary movement.<sup>98</sup>

Sections T3 (where the vomeronasal gland appears in all puppies) and T4 were mostly lined by respiratory epithelium in all puppies (Figure 3). The vomeronasal gland (organ of Jacobson) is vestigial in humans but present in mice where, as in dogs, it plays an important role in detecting pheromones from like species.<sup>98</sup> In mesaticephalic puppies, the roof of the dorsal nasal meatus was uniquely lined by olfactory epithelium forming a characteristic "olfactory cap" (Figure 3). The respiratory epithelium of Norwich Terriers was mostly associated with mucous (Goblet) than serous cells, which appeared to be uniformly distributed throughout their nasal cavity. In primates, goblet cells increase from the anterior to posterior nasal cavity but decrease in the same direction with rodents.<sup>97,98</sup> However, mesaticephalic and brachycephalic puppies had a relative abundance of serous cells in their respiratory epithelium. The relative contribution of respiratory epithelium to the entire nasal cavity in dogs is similar to primates but differs from mice. More than 50% of the nasal cavity in dogs is similar to primates but differs from mice. More than 50% of the nasal cavity of primates is lined by respiratory epithelium whereas only 46% of the nasal cavity in

mice is lined by respiratory epithelium.<sup>98,108,110</sup> In addition, our study showed that the respiratory epithelium of dogs were thicker than those of rodents. The respiratory epithelium of primates are also thicker than those of rodents.<sup>97,98,110</sup> The vast majority of respiratory epithelium was ciliated, pseudostratified and distinctly columnar.

At the level of T5, the maxillary recess, lined by respiratory epithelium, became a complete cavity associated with abundant lateral nasal glands (Figure 3). The maxillary sinus of primates and rodents are also lined by respiratory epithelium.<sup>98</sup> In addition, at this level (T5), the turbinates were most tortuous or complex in mesaticephalic puppies but relatively simple in brachycephalic and Norwich Terrier puppies (Figure 3). In all puppy breeds studied, most turbinates were lined by consecutive repetitions of olfactory and respiratory epithelia. The surface of the turbinates were characterized by olfactory epithelial lining whereas the epithelium between one turbinate and another, on the lateral wall, was mostly respiratory epithelium. The supporting (sustentacular) cells and acinar cells of the Bowman glands, both present in the olfactory epithelium of mice have an abundance of smooth endoplasmic reticulum that is involved with metabolizing xenobiotic agents, which makes them particular targets for lesions after toxic insult.<sup>97,98</sup> The ventral nasal meatus is lined by respiratory epithelium which transitions to olfactory epithelium as the ventral nasal meatus becomes continuous with the common nasal meatus, at the level of Endoturbinates IV and V. The dorsally located frontal and ethmoid sinuses were mostly lined by olfactory epithelium (Figure 3). Olfactory epithelia were distinguishable by the presence of numerous Bowman glands, nerve bundles, sustentacular cells and interposed olfactory sensory neurons.

The turbinates persisted from T5 to T6 or T7, whereas the complete roof of the choanae and nasopharyngeal meatus, which marks their rostral origin, was consistently present from T5

or T6 to T8 (Figure 3). The entirety of the choanae and nasopharyngeal meatus was strictly lined by respiratory epithelium in all puppies studied. However, the respiratory epithelium in the nasopharyngeal meatus and choanal regions remarkably had more mucous (Goblet) cells in Norwich Terriers than in mesaticephalic and brachycephalic dogs (Figure 3). Interestingly, in all puppies, there were no nasal associated lymphoid tissues (NALT) from T1-T8, indicating their absence intranasally in Norwich Terriers, mesaticephalic and brachycephalic puppies. These NALT are focal aggregates of lymphoid tissues which constitute frontline defense against inhaled antigens. A previous study that examined the posterior third of the right nasal cavity did not find any NALT and recommended that future studies section the entire nasal cavity.<sup>111</sup> Our study, which covered sections from the nasal vestibule (T1) to the nasopharyngeal meatus at the level of the soft palate (T8), confirms their absence of NALT in healthy puppies.

### **STUDY 3**

This is the first study comparing intranasal resistance in brachycephalic and mesaticephalic dogs using computational fluid dynamics (CFD). Hostnik and companions had previously used CFD to quantify nasal resistance in English Bulldogs.<sup>18</sup> However, certain limitations in their study included the variable clinical severity of the enrolled patients and a lack of normal (mesaticephalic) dogs to compare and validate CFD as a preoperative assessment tool.<sup>18</sup> Both limitations were controlled for in our study which validates CFD for the assessment of intranasal airway resistance by comparing CFD quantitative parameters in brachycephalic and mesaticephalic dogs. In addition, this study included valuable quantitative parameters

such as wall shear stress and pressure drop and compared intranasal flow patterns in different brachycephalic breeds of dogs- English bulldog, French bull dogs and pugs.

Resistance is directly proportional to pressure drop when the flow rate is constant. In addition, resistance in laminar flow increases with increase in length but exponentially decreases with increased radius (or cross sectional area), in accordance with Poiseuille's Law.<sup>112</sup> Intranasal surgical interventions that increase cross sectional areas at critical locations where there is significant pressure drop (as demonstrated by CFD) should be the surgeon's priority, as airway resistance will be considerably decreased, allowing for better nasal ventilation. Elevated wall shear stress implies that there is exacerbated friction in a repeated manner which may drive the pathophysiology of BAS. In human studies, wall shear stress causing repeated friction of the respiratory epithelium could lead to inflammation.<sup>31,113</sup> Spatiotemporal gradients of wall shear stress has been shown to increase as temperature increases, and have functional effects on effective nasal airflow in humans.<sup>114</sup> The flow pattern in French bulldogs, English bulldogs, Pugs and Mesaticephalic dogs are illustrated (Figure 4). In all dogs, there is stationary flow in the frontal sinus and maxillary recesses. This implies that the volume of air contributed by these cavities do not fully contribute to circulation in the nasal cavity. The proximal third of the nasal cavity in brachycephalic dogs was involved in dynamic flow, having the highest air velocities. The Bernoulli principle gives an inverse relationship between pressure and velocity, in laminar flow.<sup>3</sup> This implies that the distal two-thirds of the nasal cavity in brachycephalic dogs (English and French bulldogs, and pugs) is beset by very low pressure conditions that may be inimical to proper ventilation, exacerbating signs of BAS. Among mesaticephalic controls, air appears to circulate better in the distal two-thirds of the nasal airways. In fact, air

velocities are highest in the mid-nasal cavity, facilitating effective ventilation. Comparative airflow simulation between mesaticephalic and brachycephalic dogs, thus, reveal that the goal of intranasal surgical interventions should be to improve dynamic air flow (circulation) which may or may not target obvious anatomical abnormalities.

### **LIMITATIONS AND FUTURE PERSPECTIVE**

Our study revealed that among brachycephalic breeds, there is remarkable variation in intranasal radiographic anatomy in 3-D and simulated flow pattern. For generalizations across brachycephalic breeds, a study having greater sample sizes (for higher statistical power) representing many brachycephalic breeds may be required. To consistently use radiodensity (Hounsfield) thresholds across all the mesaticephalic and brachycephalic breeds in our study for easy reproducibility, our air and tissue threshold ranges minimally overlapped. This allowed us to visually include all tissue and air compartments during CT analysis (segmentation/ image reconstruction). Lastly, in our study comparing histopathological changes between brachycephalic and mesaticephalic puppies, only one breed (French Bulldog) of brachycephalic puppies was used. This is inadequate for generalizations regarding histopathological changes in brachycephalic and mesaticephalic puppies.

Further intranasal histopathological experiments will include older brachycephalic and mesaticephalic dogs to complement this study on puppies. This will elucidate age-dependent histopathological changes associated with the intranasal contribution to brachycephalic syndrome. Specific quantification of Goblet cell numbers using Alcian Blue/ Periodic Acid Schiff will validate visual observation of marked increase in Goblet cells in the respiratory

epithelium of Norwich Terrier puppies. Also, measurement of the turbinate surface area at the level of T5 (where the maxillary recess becomes completely visible) to confirm the visual observation of greater tortuosity in mesaticephalic puppies in contrast to brachycephalic and Norwich Terrier puppies. In addition, validation of obesity as a risk factor for intranasal deformities in brachycephalic dogs will be needful since increased body weight doesn't necessarily imply obesity. Our study revealed that the fraction of total air which the functional respiratory air volume constituted decreased with increased body weight. Further effort is needed to correlate intranasal deformities with CFD results and describe the impact of the former on the latter. Finally, integrating the novel CT parameters as well as CFD simulation methods for preoperative and postoperative planning and assessment of the intranasal anatomy of patients presenting with brachycephalic syndrome will help validate this clinical tool

## **CONCLUSION**

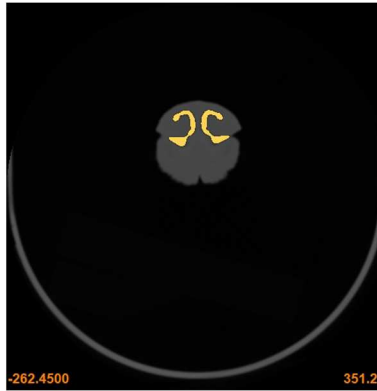
Preoperative assessment of CT scans of the nasal cavity should focus on the functional nasal volume, which comprises of the nasal cavity after excluding the frontal sinus and maxillary recess. Our study validates the use of a workflow that comprises CT analysis and CFD simulation, to investigate the extent of intranasal resistance to inform clinical or surgical treatment option. The finding of elevated Goblet cell number in the respiratory epithelium (> 50% of the entire nasal cavity) provides novel insight into the signs of brachycephalic airway syndrome (BAS) that Norwich Terriers have been reported to exhibit. The study also provides new insight as to why increased body weight correlates with exacerbated BAS. The

flow pattern and airway characteristics (shear stress, velocity and pressure profiles) has important therapeutic applications for inhalant drug administration in brachycephalic dogs.

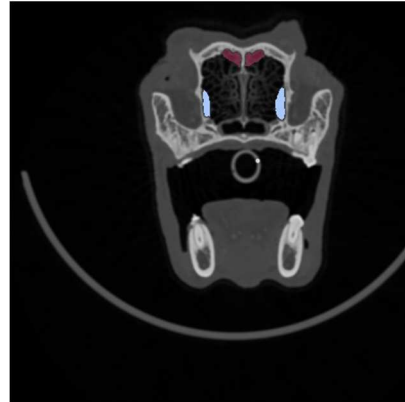
## **APPENDIX**

**Figure 2: Anatomical landmarks for preoperative assessment of CT images of the nasal cavity**

a) Rostral border of the nasal cavity



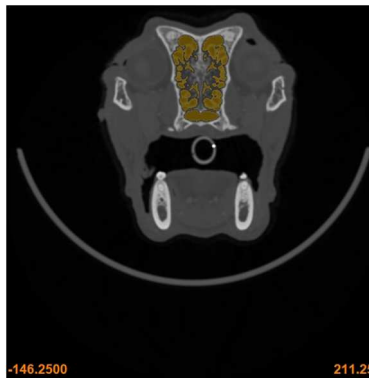
d) Total air volume = Maxillary recess (blue) + frontal sinus (pink) + functional respiratory air (black) volumes



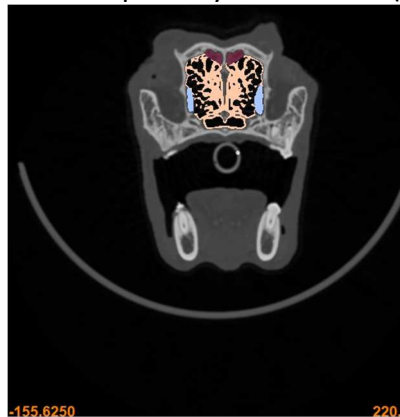
g) Cross sectional area (CSA) 1: Hard palate and nasal bone become complete



b) Caudal border of the nasal cavity at the end of the hard palate



e) Functional nasal volume = Tissue within the functional respiratory compartment (yellow) + functional respiratory air volumes (black)



h) CSA 2: Caudal border of the choanae

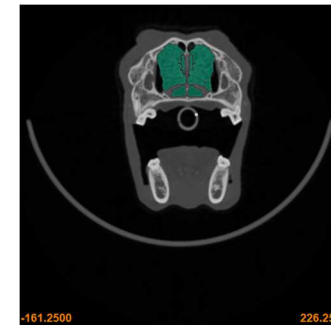
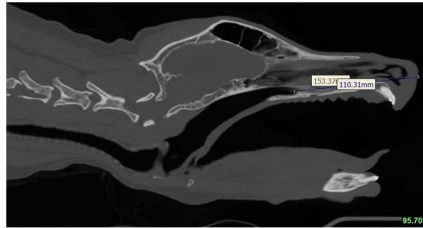


**Figure 2 (cont'd)**

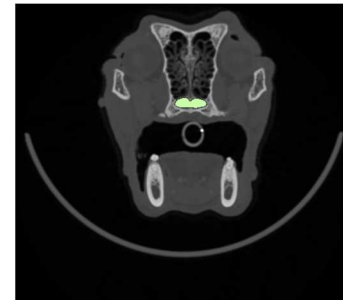
c) Caudal border of the nasal cavity beyond the hard palate



f) Length of the nasal cavity:  
Choana, sphenoid bone



i) CSA 3: Nasopharyngeal meatus



j) Presence of septal deviation

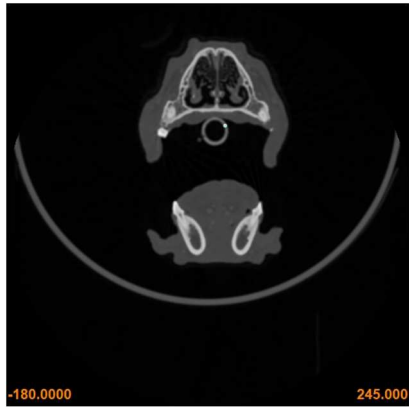


l) Presence of caudal aberrant turbinates (CAT) within the choanae



**Figure 2 (cont'd)**

k) Absence of septal deviation



m) Absence of caudal aberrant turbinates (CAT)

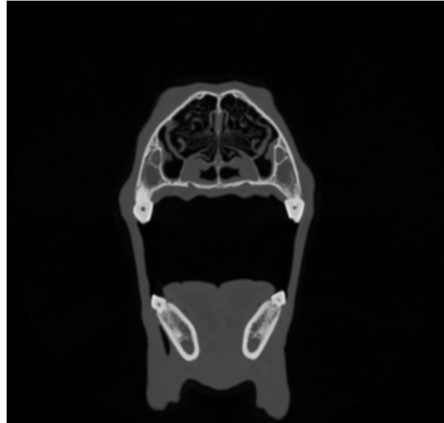
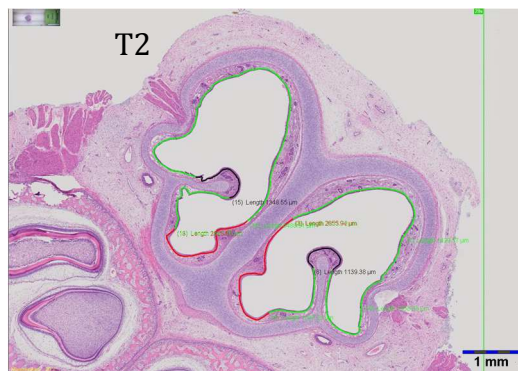
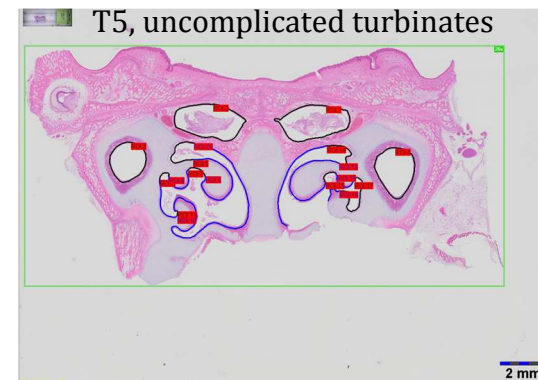
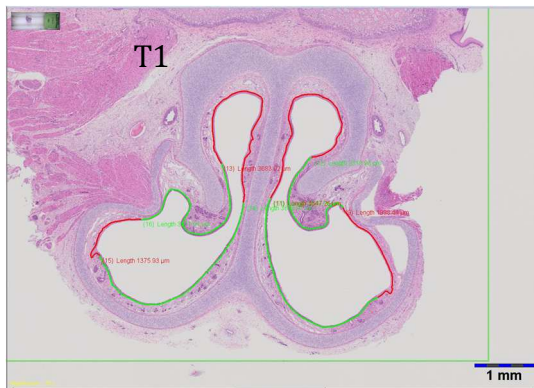


**Figure 3: The major histopathological characteristics of sections (T1-T8) of the nasal cavity in different dog breeds**

Mesaticephalic puppies

Norwich Terrier puppies

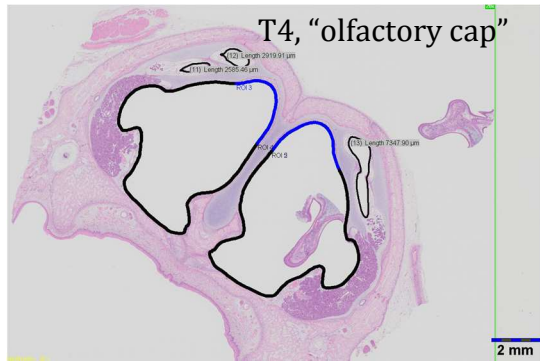
French bulldog (brachycephalic) puppies



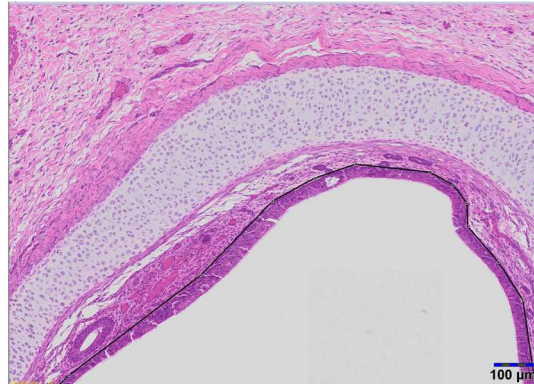
Color keys:

- Red = Squamous epithelium
- Blue = Olfactory epithelium
- Green = Transitional epithelium
- Black = Respiratory epithelium

**Figure 3 (cont'd)**



T2, higher magnification



Transition from olfactory to respiratory epithelium at the "olfactory cap"



T3, vomeronasal gland



T8, higher magnification

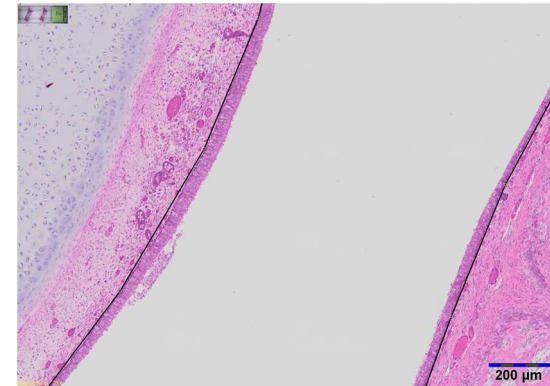


Figure 3 (cont'd)

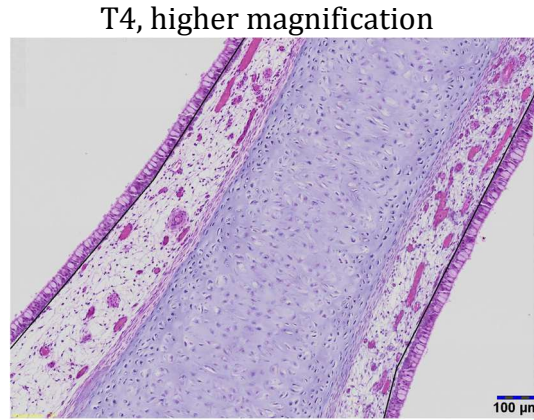
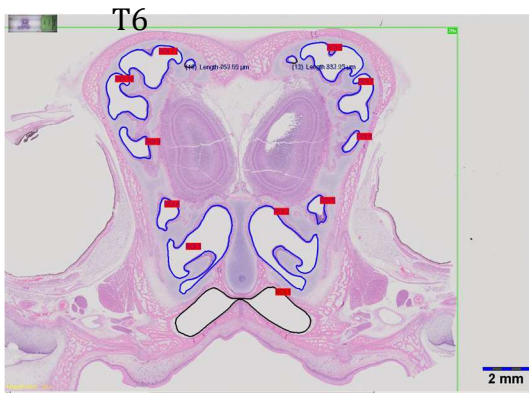
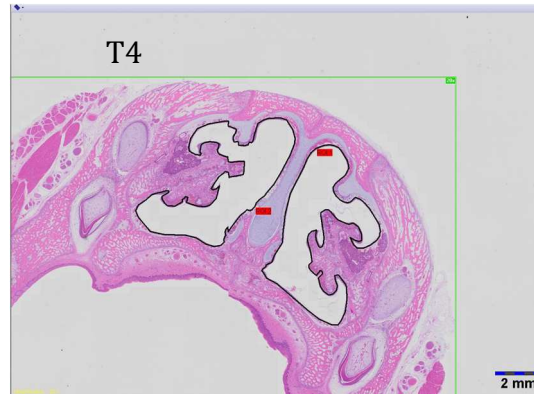
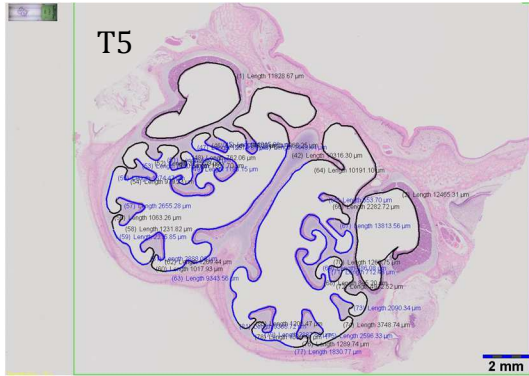
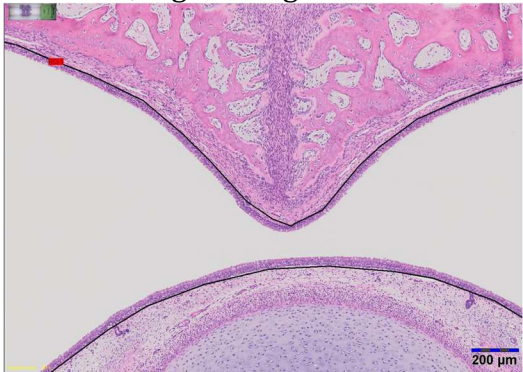


Figure 3 (cont'd)

T7



T7, higher magnification



T8



V

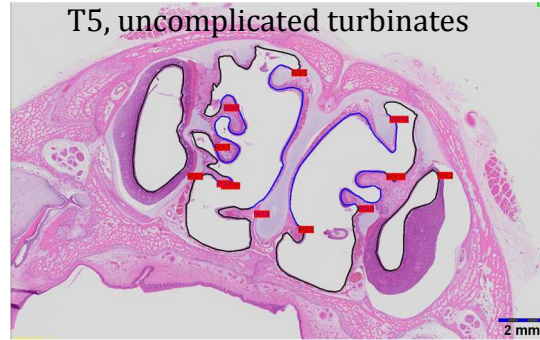


**Figure 4: Flow pattern showing velocity gradients in a mesaticephalic dog (a), French bulldog (b), English bulldog (c) and Pug (d). As velocity increases, pressure decreases (Bernoulli equation)**

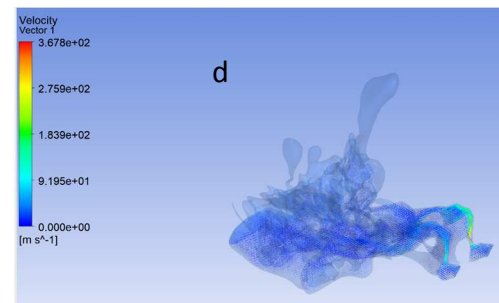
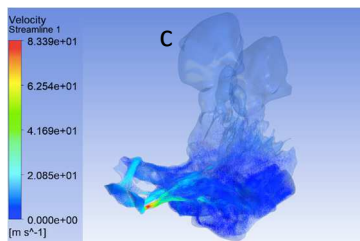
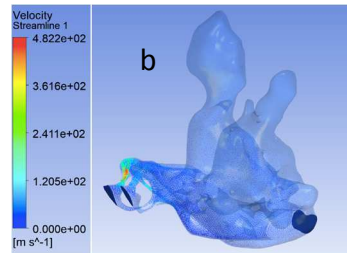
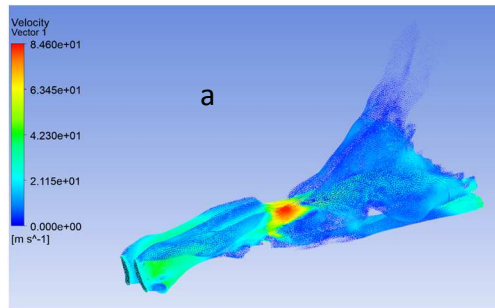


**Figure 5: Smooth 3-D image showing the inlet (a) and outlet (b) formed by the nares and nasopharyngeal meatus, respectively, in a mesaticephalic dog; inlet and outlet of a brachycephalic dog are shown in (c) and (d), respectively.**

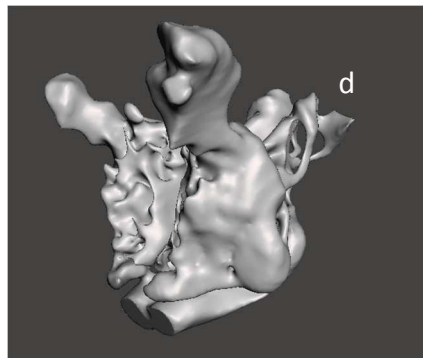
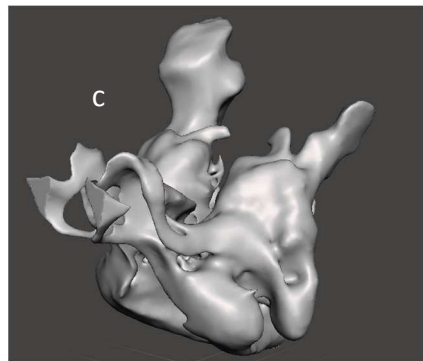
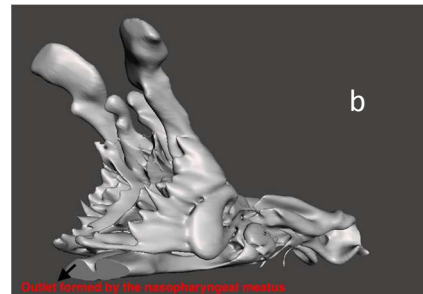
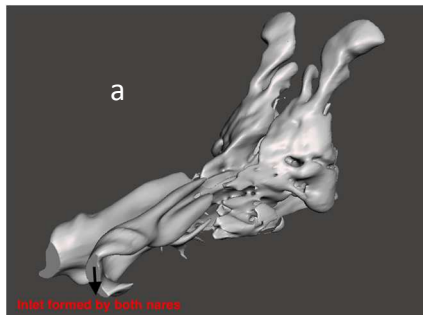
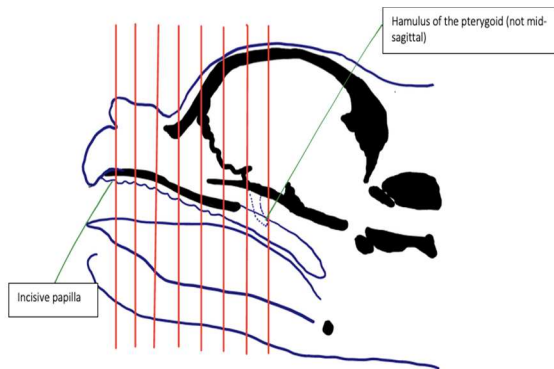


**Figure 6: Histopathological sections (T1- T8) from the incisive papilla to the soft palate at the level of the nasopharyngeal meatus**



## **REFERENCES**

## REFERENCES

- 1 Evans, H. E. & De Lahunta, A. *Miller's anatomy of the dog*. 4th edn, 26-113 (Saunders, 2012).
- 2 Packer, R. M. A., Hendricks, A. & Burn, C. C. Do dog owners perceive the clinical signs related to conformational inherited disorders as 'normal' for the breed? A potential constraint to improving canine welfare. *Animal Welfare* **21**, 81-93, doi:10.7120/096272812X13345905673809 (2012).
- 3 Koch, D. A., Arnold, S., Hubler, M. & Montavon, P. M. Brachycephalic syndrome in dogs. *Compendium on Continuing Education for the Practicing Veterinarian* **25**, 48-55 (2003).
- 4 Riecks, T. W., Birchard, S. J. & Stephens, J. A. Surgical correction of brachycephalic syndrome in dogs: 62 cases (1991-2004). *Journal of the American Veterinary Medical Association* **230**, 1324-1328, doi:10.2460/javma.230.9.1324 (2007).
- 5 Köhler, C., Menzel, A. K., Alef, M., Oechtering, G. & Kiefer, I. Comparison of soft palate thickness of normo- and brachycephalic dogs with brachycephalic airway syndrom on the basis of sagittal CT-images of the head. *Praktische Tierarzt* **97**, 981-990 (2016).
- 6 Ginn, J. A., Kumar, M. S., McKiernan, B. C. & Powers, B. E. Nasopharyngeal turbinates in brachycephalic dogs and cats. *Journal of the American Animal Hospital Association* **44**, 243-249, doi:10.5326/0440243 (2008).
- 7 Pichetto, M., Arrighi, S., Roccabianca, P. & Romussi, S. The anatomy of the dog soft palate. II. Histological evaluation of the caudal soft palate in brachycephalic breeds with grade I brachycephalic airway obstructive syndrome. *Anatomical record (Hoboken, N.J. : 2007)* **294**, 1267-1272, doi:10.1002/ar.21417 (2011).
- 8 Lodato, D. L. & Hedlund, C. S. Brachycephalic airway syndrome: pathophysiology and diagnosis. *Compendium (Yardley, PA)* **34**, E3 (2012).
- 9 Dupré, G., Findji, L. & G., O. in *Small animal soft tissue surgery* (ed E. Monnet) Ch. 19, 167 - 183 (Wiley-Blackwell, 2012).
- 10 Torrez, C. V. & Hunt, G. B. Results of surgical correction of abnormalities associated with brachycephalic airway obstruction syndrome in dogs in Australia. *The Journal of small animal practice* **47**, 150-154, doi:10.1111/j.1748-5827.2006.00059.x (2006).
- 11 Billen, F., Day, M. J. & Clercx, C. Diagnosis of pharyngeal disorders in dogs: a retrospective study of 67 cases. *The Journal of small animal practice* **47**, 122-129, doi:10.1111/j.1748-5827.2006.00032.x (2006).

- 12 Oechtering, T. H., Oechtering, G. U. & Nöller, C. Structural characteristics of the nose in brachycephalic dog breeds analysed by computed tomography. *Tierärztliche Praxis Ausgabe K: Kleintiere - Heimtiere* **35**, 177-187 (2007).
- 13 Oechtering, G. U., Pohl, S., Schlueter, C. & Schuenemann, R. A Novel Approach to Brachycephalic Syndrome. 2. Laser-Assisted Turbinectomy (LATE). *Veterinary surgery : VS* **45**, 173-181, doi:10.1111/vsu.12447 (2016).
- 14 Oechtering, G. U. *et al.* A Novel Approach to Brachycephalic Syndrome. 1. Evaluation of Anatomical Intranasal Airway Obstruction. *Veterinary surgery : VS* **45**, 165-172, doi:10.1111/vsu.12446 (2016).
- 15 Fasanella, F. J., Shivley, J. M., Wardlaw, J. L. & Givaruangsawat, S. Brachycephalic airway obstructive syndrome in dogs: 90 cases (1991-2008). *Journal of the American Veterinary Medical Association* **237**, 1048-1051, doi:10.2460/javma.237.9.1048 (2010).
- 16 Pink, J. J., Doyle, R. S., Hughes, J. M., Tobin, E. & Bellenger, C. R. Laryngeal collapse in seven brachycephalic puppies. *The Journal of small animal practice* **47**, 131-135, doi:10.1111/j.1748-5827.2006.00056.x (2006).
- 17 Huck, J. L., Stanley, B. J. & Hauptman, J. G. Technique and outcome of nares amputation (Trader's technique) in immature shih tzus. *Journal of the American Animal Hospital Association* **44**, 82-85, doi:10.5326/0440082 (2008).
- 18 Hostnik, E. T., Scansen, B. A., Zielinski, R. & Ghadiali, S. N. Quantification of nasal airflow resistance in English bulldogs using computed tomography and computational fluid dynamics. *Veterinary radiology & ultrasound : the official journal of the American College of Veterinary Radiology and the International Veterinary Radiology Association* **58**, 542-551, doi:10.1111/vru.12531 (2017).
- 19 Herdt, T. in *Textbook of Veterinary Physiology* (ed J. G. Cunningham) Ch. 28, 272-289 (Saunders, 1997).
- 20 Monnet, E. in *Textbook of Small Animal Surgery* (ed D. Slatter) Ch. 50, 808-813 (Saunders, 2003).
- 21 Clarke, D. L., Holt, D. E. & King, L. G. Partial resolution of hypoplastic trachea in six english bulldog puppies with bronchopneumonia. *Journal of the American Animal Hospital Association* **47**, 329-335, doi:10.5326/jaaha-ms-5596 (2011).
- 22 Meola, S. D. Brachycephalic airway syndrome. *Topics in companion animal medicine* **28**, 91-96, doi:10.1053/j.tcam.2013.06.004 (2013).
- 23 Club, A. K. (2019).

- 24 Hendricks, J. C. Brachycephalic Airway Syndrome. *Veterinary Clinics of North America: Small Animal Practice* **22**, 1145-1153, doi:10.1016/S0195-5616(92)50306-0 (1992).
- 25 Johnson, L. R. *et al.* Upper airway obstruction in Norwich Terriers: 16 cases. *Journal of veterinary internal medicine* **27**, 1409-1415, doi:10.1111/jvim.12206 (2013).
- 26 Grand, J. G. & Bureau, S. Structural characteristics of the soft palate and meatus nasopharyngeus in brachycephalic and non-brachycephalic dogs analysed by CT. *The Journal of small animal practice* **52**, 232-239, doi:10.1111/j.1748-5827.2011.01047.x (2011).
- 27 Poncet, C. M., Dupre, G. P., Freiche, V. G. & Bouvy, B. M. Long-term results of upper respiratory syndrome surgery and gastrointestinal tract medical treatment in 51 brachycephalic dogs. *The Journal of small animal practice* **47**, 137-142, doi:10.1111/j.1748-5827.2006.00057.x (2006).
- 28 Koch, D. A., Rosaspina, M., Wiestner, T., Arnold, S. & Montavon, P. M. Comparative investigations on the upper respiratory tract in Norwich terriers, brachycephalic and mesaticephalic dogs. *Schweizer Archiv fur Tierheilkunde* **156**, 119-124, doi:10.1024/0036-7281/a000561 (2014).
- 29 Kirberger, R. M. *et al.* Stenotic nasopharyngeal dysgenesis in the dachshund: seven cases (2002-2004). *Journal of the American Animal Hospital Association* **42**, 290-297, doi:10.5326/0420290 (2006).
- 30 Auger, M., Alexander, K., Beauchamp, G. & Dunn, M. Use of CT to evaluate and compare intranasal features in brachycephalic and normocephalic dogs. *The Journal of small animal practice* **57**, 529-536, doi:10.1111/jsap.12541 (2016).
- 31 Chen, X. B., Lee, H. P., Chong, V. F. & Wang de, Y. Assessment of septal deviation effects on nasal air flow: a computational fluid dynamics model. *The Laryngoscope* **119**, 1730-1736, doi:10.1002/lary.20585 (2009).
- 32 Lee, D. C. *et al.* Anatomical analysis of nasal obstruction: nasal cavity of patients complaining of stuffy nose. *The Laryngoscope* **123**, 1381-1384, doi:10.1002/lary.23841 (2013).
- 33 Vilaplana Grosso, F., Haar, G. T. & Boroffka, S. A. Gender, weight, and age effects on prevalence of caudal aberrant nasal turbinates in clinically healthy English Bulldogs: A computed tomographic study and classification. *Veterinary radiology & ultrasound : the official journal of the American College of Veterinary Radiology and the International Veterinary Radiology Association* **56**, 486-493, doi:10.1111/vru.12249 (2015).

- 34 De Lorenzi, D., Bertoncetto, D. & Drigo, M. Bronchial abnormalities found in a consecutive series of 40 brachycephalic dogs. *Journal of the American Veterinary Medical Association* **235**, 835-840, doi:10.2460/javma.235.7.835 (2009).
- 35 Robinson, N. E. Airway physiology. *The Veterinary clinics of North America. Small animal practice* **22**, 1043-1064 (1992).
- 36 Ohnishi, T. & Ogura, J. H. Partitioning of pulmonary resistance in the dog. *The Laryngoscope* **79**, 1847-1878, doi:10.1288/00005537-196911000-00001 (1969).
- 37 Emmerson, T. Brachycephalic obstructive airway syndrome: a growing problem. *The Journal of small animal practice* **55**, 543-544, doi:10.1111/jsap.12286 (2014).
- 38 Ayappa, I. & Rapoport, D. M. The upper airway in sleep: physiology of the pharynx. *Sleep medicine reviews* **7**, 9-33 (2003).
- 39 White, D. P., Lombard, R. M., Cadieux, R. J. & Zwillich, C. W. Pharyngeal resistance in normal humans: influence of gender, age, and obesity. *Journal of applied physiology (Bethesda, Md. : 1985)* **58**, 365-371, doi:10.1152/jappl.1985.58.2.365 (1985).
- 40 Goding, G. S., Jr. *et al.* Relief of upper airway obstruction with hypoglossal nerve stimulation in the canine. *The Laryngoscope* **108**, 162-169 (1998).
- 41 Yokoba, M., Hawes, H. G. & Easton, P. A. Geniohyoid muscle function in awake canines. *Journal of applied physiology (Bethesda, Md. : 1985)* **95**, 810-817, doi:10.1152/japplphysiol.00332.2002 (2003).
- 42 Hobson, H. P. Brachycephalic syndrome. *Seminars in veterinary medicine and surgery (small animal)* **10**, 109-114 (1995).
- 43 Salguero, R., Herrtage, M., Holmes, M., Mannion, P. & Ladlow, J. Comparison between computed tomographic characteristics of the middle ear in nonbrachycephalic and brachycephalic dogs with obstructive airway syndrome. *Veterinary radiology & ultrasound : the official journal of the American College of Veterinary Radiology and the International Veterinary Radiology Association* **57**, 137-143, doi:10.1111/vru.12337 (2016).
- 44 Mellema, M. & Hoareau, G. in *Journal of veterinary internal medicine* Vol. 28 1418-1423 (2014).
- 45 Schmidt, M. J., Wigger, A., Jawinski, S., Golla, T. & Kramer, M. Ultrasonographic appearance of the craniocervical junction in normal brachycephalic dogs and dogs with caudal occipital (Chiari-like) malformation. *Veterinary radiology & ultrasound : the official journal of the American College of Veterinary Radiology and the International Veterinary Radiology Association* **49**, 472-476 (2008).

- 46 Gutierrez-Quintana, R. *et al.* A proposed radiographic classification scheme for congenital thoracic vertebral malformations in brachycephalic "screw-tailed" dog breeds. *Veterinary radiology & ultrasound : the official journal of the American College of Veterinary Radiology and the International Veterinary Radiology Association* **55**, 585-591, doi:10.1111/vru.12172 (2014).
- 47 Christmas, R. E. Common ocular problems of Shin Tzu dogs. *The Canadian veterinary journal = La revue veterinaire canadienne* **33**, 390-393 (1992).
- 48 Farrell, L. L., Schoenebeck, J. J., Wiener, P., Clements, D. N. & Summers, K. M. in *Canine Genet Epidemiol* Vol. 2 (2015).
- 49 Blocker, T. & Van Der Woerdt, A. A comparison of corneal sensitivity between brachycephalic and Domestic Short-haired cats. *Veterinary ophthalmology* **4**, 127-130 (2001).
- 50 Parker, J. D. *et al.* Acute and chronic effects of airway obstruction on canine left ventricular performance. *American journal of respiratory and critical care medicine* **160**, 1888-1896, doi:10.1164/ajrccm.160.6.9807074 (1999).
- 51 Roedler, F. S., Pohl, S. & Oechtering, G. U. How does severe brachycephaly affect dog's lives? Results of a structured preoperative owner questionnaire. *Veterinary journal (London, England : 1997)* **198**, 606-610, doi:10.1016/j.tvjl.2013.09.009 (2013).
- 52 Caccamo, R., Buracco, P., La Rosa, G., Cantatore, M. & Romussi, S. in *BMC Vet Res* Vol. 10 12 (2014).
- 53 Stadler, K., Hartman, S., Matheson, J. & O'Brien, R. Computed tomographic imaging of dogs with primary laryngeal or tracheal airway obstruction. *Veterinary radiology & ultrasound : the official journal of the American College of Veterinary Radiology and the International Veterinary Radiology Association* **52**, 377-384, doi:10.1111/j.1740-8261.2011.01816.x (2011).
- 54 Schmidt, M. J., Neumann, A. C., Amort, K. H., Failing, K. & Kramer, M. Cephalometric measurements and determination of general skull type of Cavalier King Charles Spaniels. *Veterinary radiology & ultrasound : the official journal of the American College of Veterinary Radiology and the International Veterinary Radiology Association* **52**, 436-440, doi:10.1111/j.1740-8261.2011.01825.x (2011).
- 55 Heidenreich, D., Gradner, G., Kneissl, S. & Dupre, G. Nasopharyngeal Dimensions From Computed Tomography of Pugs and French Bulldogs With Brachycephalic Airway Syndrome. *Veterinary surgery : VS* **45**, 83-90, doi:10.1111/vsu.12418 (2016).
- 56 Rutherford, L., Beever, L., Bruce, M. & Ter Haar, G. Assessment of computed tomography derived cricoid cartilage and tracheal dimensions to evaluate degree of cricoid narrowing in brachycephalic dogs. *Veterinary radiology & ultrasound : the*

- official journal of the American College of Veterinary Radiology and the International Veterinary Radiology Association* **58**, 634-646, doi:10.1111/vru.12526 (2017).
- 57 Kaye, B. M., Boroffka, S. A., Haagsman, A. N. & Ter Haar, G. COMPUTED TOMOGRAPHIC, RADIOGRAPHIC, AND ENDOSCOPIC TRACHEAL DIMENSIONS IN ENGLISH BULLDOGS WITH GRADE 1 CLINICAL SIGNS OF BRACHYCEPHALIC AIRWAY SYNDROME. *Veterinary radiology & ultrasound : the official journal of the American College of Veterinary Radiology and the International Veterinary Radiology Association* **56**, 609-616, doi:10.1111/vru.12277 (2015).
- 58 Craven, B. A. *et al.* Reconstruction and morphometric analysis of the nasal airway of the dog (*Canis familiaris*) and implications regarding olfactory airflow. *Anatomical record (Hoboken, N.J. : 2007)* **290**, 1325-1340, doi:10.1002/ar.20592 (2007).
- 59 Slaats, M. A. *et al.* Upper airway imaging in pediatric obstructive sleep apnea syndrome. *Sleep medicine reviews* **21**, 59-71, doi:10.1016/j.smrv.2014.08.001 (2015).
- 60 Findji, L. & Dupré, G. Folded flap palatoplasty for treatment of elongated soft palates in 55 dogs. *Wiener Tierärztliche Monatsschrift* **95**, 56-63 (2008).
- 61 Liu, N. C. *et al.* Outcomes and prognostic factors of surgical treatments for brachycephalic obstructive airway syndrome in 3 breeds. *Veterinary surgery : VS* **46**, 271-280, doi:10.1111/vsu.12608 (2017).
- 62 Schmiedt, C. W. in *Veterinary Surgery: Small Animal* Vol. 2 (eds Spencer A. Johnston & Karen M. Tobias) Ch. 99, 1919 (Elsevier, 2017).
- 63 Kealy, J. K., McAllister, H. & Graham, J. P. in *Diagnostic Radiology and Ultrasonography of the Dog and Cat (FIFTH EDITION)* 447-541 (W.B. Saunders, 2011).
- 64 Wisner, E. & Zwingenberger, A. *Atlas of small animal CT and MRI*. 5th edn, 3 (Wiley Blackwell, 2015).
- 65 Schuenemann, R. & Oechtering, G. U. Inside the brachycephalic nose: intranasal mucosal contact points. *Journal of the American Animal Hospital Association* **50**, 149-158, doi:10.5326/jaaha-ms-5991 (2014).
- 66 Schuenemann, R. & Oechtering, G. Inside the brachycephalic nose: conchal regrowth and mucosal contact points after laser-assisted turbinectomy. *Journal of the American Animal Hospital Association* **50**, 237-246, doi:10.5326/jaaha-ms-6086 (2014).
- 67 Dunie-Merigot, A., Bouvy, B. & Poncet, C. Comparative use of CO<sub>2</sub> laser, diode laser and monopolar electrocautery for resection of the soft palate in dogs with brachycephalic airway obstructive syndrome. *The Veterinary record* **167**, 700-704, doi:10.1136/vr.c5107 (2010).

- 68 Lippert, J. P. *et al.* [Geometry and function of the dog nose: how does function change when form of the nose is changed?]. *Pneumologie (Stuttgart, Germany)* **64**, 452-453, doi:10.1055/s-0030-1255515 (2010).
- 69 Hirt, R. A., Leinker, S., Mosing, M. & Wiederstein, I. Comparison of barometric whole body plethysmography and its derived parameter enhanced pause (PENH) with conventional respiratory mechanics in healthy Beagle dogs. *Veterinary journal (London, England : 1997)* **176**, 232-239, doi:10.1016/j.tvjl.2007.05.025 (2008).
- 70 Bernaerts, F. *et al.* Description of original endoscopic findings and respiratory functional assessment using barometric whole-body plethysmography in dogs suffering from brachycephalic airway obstruction syndrome. *Veterinary journal (London, England : 1997)* **183**, 95-102, doi:10.1016/j.tvjl.2008.09.009 (2010).
- 71 Grutzenmacher, S., Lang, C. & Mlynski, G. The combination of acoustic rhinometry, rhinoresistometry and flow simulation in noses before and after turbinate surgery: a model study. *ORL; journal for oto-rhino-laryngology and its related specialties* **65**, 341-347, doi:10.1159/000076052 (2003).
- 72 Davis, S. S. & Eccles, R. Nasal congestion: mechanisms, measurement and medications. Core information for the clinician. *Clinical otolaryngology and allied sciences* **29**, 659-666, doi:10.1111/j.1365-2273.2004.00885.x (2004).
- 73 Lawson, M. J., Craven, B. A., Paterson, E. G. & Settles, G. S. A computational study of odorant transport and deposition in the canine nasal cavity: implications for olfaction. *Chemical senses* **37**, 553-566, doi:10.1093/chemse/bjs039 (2012).
- 74 Craven, B. A., Paterson, E. G. & Settles, G. S. in *J R Soc Interface* Vol. 7 933-943 (2010).
- 75 Craven, B. A., Paterson, E. G., Settles, G. S. & Lawson, M. J. Development and verification of a high-fidelity computational fluid dynamics model of canine nasal airflow. *Journal of biomechanical engineering* **131**, 091002, doi:10.1115/1.3148202 (2009).
- 76 Rakesh, V., Rakesh, N. G., Datta, A. K., Cheetham, J. & Pease, A. P. Development of equine upper airway fluid mechanics model for Thoroughbred racehorses. *Equine veterinary journal* **40**, 272-279, doi:10.2746/042516408x281216 (2008).
- 77 Vos, W. *et al.* Correlation between severity of sleep apnea and upper airway morphology based on advanced anatomical and functional imaging. *Journal of biomechanics* **40**, 2207-2213, doi:10.1016/j.jbiomech.2006.10.024 (2007).
- 78 Nie, P. *et al.* Computational fluid dynamics simulation of the upper airway of obstructive sleep apnea syndrome by Muller maneuver. *Journal of Huazhong University of Science and Technology. Medical sciences = Hua zhong ke ji da xue xue bao. Yi xue Ying De wen ban = Huazhong keji daxue xuebao. Yixue Yingdewen ban* **35**, 464-468, doi:10.1007/s11596-015-1454-x (2015).

- 79 Tan, J. *et al.* Numerical simulation of normal nasal cavity airflow in Chinese adult: a computational flow dynamics model. *European archives of oto-rhino-laryngology : official journal of the European Federation of Oto-Rhino-Laryngological Societies (EUFOS) : affiliated with the German Society for Oto-Rhino-Laryngology - Head and Neck Surgery* **269**, 881-889, doi:10.1007/s00405-011-1771-z (2012).
- 80 Kim, T. *et al.* Change in the Upper Airway of Patients With Obstructive Sleep Apnea Syndrome Using Computational Fluid Dynamics Analysis: Conventional Maxillomandibular Advancement Versus Modified Maxillomandibular Advancement With Anterior Segmental Setback Osteotomy. *The Journal of craniofacial surgery* **26**, e765-770, doi:10.1097/scs.0000000000002209 (2015).
- 81 Van Holsbeke, C. *et al.* Functional respiratory imaging as a tool to assess upper airway patency in children with obstructive sleep apnea. *Sleep medicine* **14**, 433-439, doi:10.1016/j.sleep.2012.12.005 (2013).
- 82 Mylavarapu, G. *et al.* Validation of computational fluid dynamics methodology used for human upper airway flow simulations. *Journal of biomechanics* **42**, 1553-1559, doi:10.1016/j.jbiomech.2009.03.035 (2009).
- 83 Iwasaki, T. *et al.* The effect of rapid maxillary expansion on pharyngeal airway pressure during inspiration evaluated using computational fluid dynamics. *International journal of pediatric otorhinolaryngology* **78**, 1258-1264, doi:10.1016/j.ijporl.2014.05.004 (2014).
- 84 Yu, C. C. *et al.* Computational fluid dynamics study of the inspiratory upper airway and clinical severity of obstructive sleep apnea. *The Journal of craniofacial surgery* **23**, 401-405, doi:10.1097/SCS.0b013e318240feed (2012).
- 85 Fletcher, A. *et al.* The effect of geniglossal advancement on airway flow using a computational flow dynamics model. *The Laryngoscope* **123**, 3227-3232, doi:10.1002/lary.24203 (2013).
- 86 Sittitavornwong, S. *et al.* Computational fluid dynamic analysis of the posterior airway space after maxillomandibular advancement for obstructive sleep apnea syndrome. *Journal of oral and maxillofacial surgery : official journal of the American Association of Oral and Maxillofacial Surgeons* **71**, 1397-1405, doi:10.1016/j.joms.2013.02.022 (2013).
- 87 Iwasaki, T. *et al.* Tongue posture improvement and pharyngeal airway enlargement as secondary effects of rapid maxillary expansion: a cone-beam computed tomography study. *American journal of orthodontics and dentofacial orthopedics : official publication of the American Association of Orthodontists, its constituent societies, and the American Board of Orthodontics* **143**, 235-245, doi:10.1016/j.ajodo.2012.09.014 (2013).

- 88 De Backer, J. W. *et al.* Functional imaging using computational fluid dynamics to predict treatment success of mandibular advancement devices in sleep-disordered breathing. *Journal of biomechanics* **40**, 3708-3714, doi:10.1016/j.jbiomech.2007.06.022 (2007).
- 89 Pichetto, M., Arrighi, S., Gobbetti, M. & Romussi, S. The anatomy of the dog soft palate. III. Histological evaluation of the caudal soft palate in brachycephalic neonates. *Anatomical record (Hoboken, N.J. : 2007)* **298**, 618-623, doi:10.1002/ar.23054 (2015).
- 90 Okano, M. & Sugawa, Y. [Ultrastructure of the respiratory mucous epithelium of the canine nasal cavity]. *Arch Histol Jpn* **26**, 1-21 (1965).
- 91 Adams, D. R. & Hotchkiss, D. K. The canine nasal mucosa. *Anat Histol Embryol* **12**, 109-125 (1983).
- 92 Laurenson, M. P. *et al.* Computed tomography of the pharynx in a closed vs. open mouth position. *Veterinary radiology & ultrasound : the official journal of the American College of Veterinary Radiology and the International Veterinary Radiology Association* **52**, 357-361, doi:10.1111/j.1740-8261.2011.01805.x (2011).
- 93 Liu, N. C. *et al.* Endotracheal tube placement during computed tomography of brachycephalic dogs alters upper airway dimensional measurements. *Veterinary radiology & ultrasound : the official journal of the American College of Veterinary Radiology and the International Veterinary Radiology Association* **59**, 289-304, doi:10.1111/vru.12590 (2018).
- 94 Cook, W. R. Observations on the Upper Respiratory Tract of the Dog and Cat. *J. Small Anim. Pract.* **5**, 309-329, doi:10.1111/j.1748-5827.1964.tb04259.x (1964).
- 95 Harcourt-Brown, N. Rhinoscopy in the dog. 1. Anatomy and techniques. *In Practice* **28**, 170-175, doi:10.1136/inpract.28.4.170 (2006).
- 96 Koch, D. *et al.* Proposal for a new radiological index to determine skull conformation in the dog. *Schweizer Archiv fur Tierheilkunde* **154**, 217-220, doi:10.1024/0036-7281/a000331 (2012).
- 97 Harkema, J. R., Carey, S. A. & Wagner, J. G. The nose revisited: a brief review of the comparative structure, function, and toxicologic pathology of the nasal epithelium. *Toxicologic pathology* **34**, 252-269, doi:10.1080/01926230600713475 (2006).
- 98 Harkema, J. R., Carey, S. A., Wagner, J. G., Dintzis, S. M. & Liggitt, D. in *Comparative Anatomy and Histology: a Mouse and Human Atlas* (eds P. M. Treuting & S. M. Dintzis) 71-94 (Elsevier Academic Press Inc, 2011).
- 99 Kimbell, J., Frank, D., Laud, P., Garcia, G. & Rhee, J. Changes in nasal airflow and heat transfer correlate with symptom improvement after surgery for nasal obstruction. *Journal of biomechanics* **46**, 2634-2643, doi:10.1016/j.jbiomech.2013.08.007 (2013).

- 100 Benavides, K., Rozanski, E., Anastasio, J. D. & Bedenice, D. in *Journal of veterinary internal medicine* Vol. 33 208-211 (2019).
- 101 Skinner, A. P., Pachnicke, S., Lakatos, A., Franklin, R. J. & Jeffery, N. D. Nasal and frontal sinus mucosa of the adult dog contain numerous olfactory sensory neurons and ensheathing glia. *Res Vet Sci* **78**, 9-15, doi:10.1016/j.rvsc.2004.05.010 (2005).
- 102 Manens, J. *et al.* Effects of obesity on lung function and airway reactivity in healthy dogs. *Veterinary journal (London, England : 1997)* **193**, 217-221, doi:10.1016/j.tvjl.2011.10.013 (2012).
- 103 Zerah, F. *et al.* Effects of obesity on respiratory resistance. *Chest* **103**, 1470-1476, doi:10.1378/chest.103.5.1470 (1993).
- 104 Packer, R. M. A., Hendricks, A. & Burn, C. C. in *PLoS One* Vol. 10 (2015).
- 105 Bach, J. F. *et al.* Association of expiratory airway dysfunction with marked obesity in healthy adult dogs. *Am J Vet Res* **68**, 670-675, doi:10.2460/ajvr.68.6.670 (2007).
- 106 Harkema, J. R., Plopper, C. G., Hyde, D. M., St George, J. A. & Dungworth, D. L. Effects of an ambient level of ozone on primate nasal epithelial mucosubstances. Quantitative histochemistry. *Am J Pathol* **127**, 90-96 (1987).
- 107 Harkema, J. R. *et al.* Response of the macaque nasal epithelium to ambient levels of ozone. A morphologic and morphometric study of the transitional and respiratory epithelium. *Am J Pathol* **128**, 29-44 (1987).
- 108 Gross, E. A., Swenberg, J. A., Fields, S. & Popp, J. A. Comparative morphometry of the nasal cavity in rats and mice. *J Anat* **135**, 83-88 (1982).
- 109 Sorokin, S. P. in *Cell and Tissue Biology: A Textbook of Histology* (ed L. Weiss) 751-814 (Urban & Schwarzenberg, 1988).
- 110 Carey, S. A. *et al.* Three-dimensional mapping of ozone-induced injury in the nasal airways of monkeys using magnetic resonance imaging and morphometric techniques. *Toxicologic pathology* **35**, 27-40, doi:10.1080/01926230601072343 (2007).
- 111 Peeters, D., Day, M. J., Farnir, F., Moore, P. & Clercx, C. Distribution of leucocyte subsets in the canine respiratory tract. *J Comp Pathol* **132**, 261-272, doi:10.1016/j.jcpa.2004.10.003 (2005).
- 112 Moulin, D., Bertrand, J. M., Buts, J. P., Nyakabasa, M. & Otte, J. B. Upper airway lesions in children after accidental ingestion of caustic substances. *J Pediatr* **106**, 408-410 (1985).

- 113 Garcia, G. J., Bailie, N., Martins, D. A. & Kimbell, J. S. Atrophic rhinitis: a CFD study of air conditioning in the nasal cavity. *Journal of applied physiology (Bethesda, Md. : 1985)* **103**, 1082-1092, doi:10.1152/jappphysiol.01118.2006 (2007).
- 114 Elad, D., Naftali, S., Rosenfeld, M. & Wolf, M. Physical stresses at the air-wall interface of the human nasal cavity during breathing. *Journal of applied physiology (Bethesda, Md. : 1985)* **100**, 1003-1010, doi:10.1152/jappphysiol.01049.2005 (2006).